

THE UNCERTAINTY ELIMINATION IN DISCRETE TOPOLOGY OPTIMIZATION OF
COMPLIANT MECHANISMS

A Thesis

by

SATYA RAVITEJA KANDALA

Submitted to the College of Graduate Studies
Texas A&M University-Kingsville
in partial fulfillment of the requirements for the degree of

MASTER OF SCIENCE

December 2013

Major Subject: Mechanical Engineering

UMI Number: 1550683

All rights reserved

INFORMATION TO ALL USERS

The quality of this reproduction is dependent upon the quality of the copy submitted.

In the unlikely event that the author did not send a complete manuscript and there are missing pages, these will be noted. Also, if material had to be removed, a note will indicate the deletion.



UMI 1550683

Published by ProQuest LLC (2014). Copyright in the Dissertation held by the Author.

Microform Edition © ProQuest LLC.

All rights reserved. This work is protected against unauthorized copying under Title 17, United States Code



ProQuest LLC.
789 East Eisenhower Parkway
P.O. Box 1346
Ann Arbor, MI 48106 - 1346

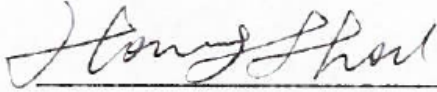
THE UNCERTAINTY ELIMINATION IN DISCRETE TOPOLOGY OPTIMIZATION OF
COMPLIANT MECHANISMS

A Thesis

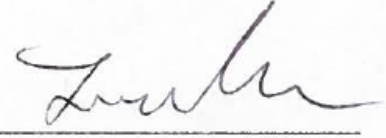
by

SATYA RAVITEJA KANDALA

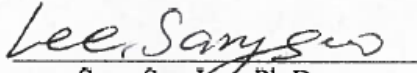
Approved as to style and content by:



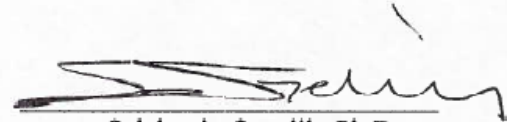
Hong Zhou, Ph.D.
(Chairman of Committee)



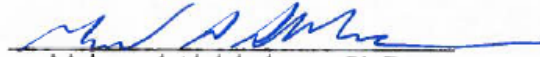
Joon-Yeoul Oh Ph.D.
(Committee Member)



Sang Soo Lee, Ph.D.
(Committee Member)



Selahattin Ozcelik, Ph.D.
(Chairman of Department)



Mohamed Abdelrahman, Ph.D.
(Associate Vice President for Research and Dean of Graduate Studies)

December 2013

ABSTRACT

The Uncertainty Elimination in Discrete Topology Optimization of Compliant Mechanisms

(December 2013)

Satya Raviteja Kandala, B.Tech, JNT University, India

Chairman of Advisory Committee: Dr. Hong Zhou

The uncertainty in topology optimization leads to ambiguity caused by different topology solutions. This uncertainty is caused by either having point connections or grey cells which are eliminated by using hybrid discretization model for discrete topology optimization. Mesh dependence also contributes to topology uncertainty. When the design domain of a topology is discretized differently, its solution depends on the type of discretization which leads to uncertainty caused by mesh dependence. To address the problem of mesh dependence, the genus based topology optimization strategy is introduced in this thesis. This approach deals with controlling of the genus of an optimized compliant mechanism in the process of optimizing the topology. There is no uncertainty caused by mesh dependence when this strategy is implemented with hybrid discretization for topology optimization. An example is considered to demonstrate the introduced approach.

ACKNOWLEDGEMENT

I would like to express my sincere gratitude to Dr. Hong Zhou, Advisor for this Graduate Thesis, for his immense patience, expert guidance and valuable suggestions throughout my thesis and course work.

My sincere thanks to Dr. Sang Soo Lee and Dr. Joon-Yeoul Oh, my committee members for their guidance and extended help to support my course work.

I would like to thank the entire faculty of Department of Mechanical Engineering for their support and also for giving me immense knowledge from my course work in this university.

My special thanks and my sincere gratitude to Texas A & M University, Kingsville and to the Dean of Graduate Studies Dr. Mohamed Abdelrahman.

Finally, I would also like to thank my parents and my friends for their constant encouragement and inspiration that kept me charged while pursuing my Master's degree without whom it would have never been possible.

TABLE OF CONTENTS

	Page
ABSTRACT	iii
ACKNOWLEDGEMENT	iv
TABLE OF CONTENTS.....	v
LIST OF FIGURES	viii
LIST OF TABLES	xiv
CHAPTER I.....	1
INTRODUCTION	1
1.1 Topology Optimization of Compliant Mechanisms.....	1
1.2 Criteria for Designing Mechanisms	2
1.3 Advantages of Compliant Mechanisms.....	3
1.4 The Degree of Genus.....	3
1.5 Current Research Situation.....	4
1.6 Research, Motivation and Approach.....	5
1.7 Thesis Organization.....	6
CHAPTER II.....	7

THE DOG CONTROL STRATEGY	7
2.1 Discretization of the Design Domain	7
2.2 Computing the DOG	9
2.2.1 Discretizing the design domain	9
2.2.2 Removal of dangling and redundant Cells	10
2.2.3 Flipping the design cells	12
2.2.4 Counting the Number of holes in the Topology	14
CHAPTER III	16
TOPOLOGY OPTIMIZATION FORMULATION	16
CHAPTER IV	18
OPTIMIZATION ALGORITHM	18
4.1 Criteria for Finding Connectivity of Design Cells	19
4.2 Generation of Pool for Selecting Optimum Topology	19
CHAPTER V	21
TOPOLOGY OPTIMIZATION EXAMPLES	21
5.1 Compliant Displacement Amplifier	21
5.1.1 The topology optimization results with DOG of 5	24

5.1.2	The topology optimization results with DOG of 6	26
5.1.3	The topology optimization results with DOG of 7	28
5.1.4	The topology optimization results with DOG of 8	31
CHAPTER VI		34
RESULTS FROM SOLID WORKS		34
6.1	Results for DOG 5	34
6.2	Results for DOG 6	38
6.3	Results for DOG 7	43
6.4	Results for DOG 8	48
6.5	Results without DOG Strategy	53
CHAPTER VII		57
CONCLUSIONS AND FUTURE RESEARCH		57
7.1	Conclusions	57
7.2	Future Research	58
REFERENCES		59
VITA		61

LIST OF FIGURES

	Page
FIGURE 2.1 A SUBDIVIDED QUADRILATERAL DESIGN CELL WITH ITS INNER AND CORNER DESIGN CELLS	7
FIGURE 2.2 THE FOUR CORNER TRIANGLES BETWEEN TWO NEIGHBORING QUADRILATERAL DESIGN CELLS.....	8
FIGURE 2.3 TWO SOLID NEIGHBORING QUADRILATERAL DESIGN CELLS IN DIFFERENT DIRECTIONS	9
FIGURE 2.4 THE QUADRILATERAL DESIGN CELLS IN HYBRID DISCRETIZATION MODEL.....	9
FIGURE 2.5 THE SUBDIVIDED TRIANGULAR ANALYSIS CELLS IN HYBRID DISCRETIZATION MODEL.....	10
FIGURE 2.6 THE QUADRILATERAL DESIGN CELLS OF A TOPOLOGY.....	10
FIGURE 2.7 THE TRIANGULAR ANALYSIS CELLS OF A TOPOLOGY.....	11
FIGURE 2.8 THE TOPOLOGY OF FIGURE 2.5 AFTER REMOVING DANGLING AND REDUNDANT DESIGN CELLS.....	12
FIGURE 2.9 THE FLIPPED TOPOLOGY OF FIGURE 2.6 IN THE DISCRETIZED DESIGN DOMAIN	13
FIGURE 2.10 THE TOPOLOGY OF FIGURE 2.7 AFTER REMOVING SOLID DESIGN CELLS THAT ARE CONNECTED TO ANY SOLID BOUNDARY DESIGN CELL	14

FIGURE 2.11 THE TOPOLOGY OF FIGURE 2.7 AFTER REMOVING SOLID DESIGN CELLS THAT ARE CONNECTED TO ANY SOLID BOUNDARY DESIGN CELL	14
FIGURE 2.12 THE TOPOLOGY OF FIGURE 2.8 AFTER REMOVING THE SOLID DESIGN CELLS THAT FORM THE FIRST HOLE	15
FIGURE 2.13 THE TOPOLOGY AFTER REMOVING THE SOLID DESIGN CELLS THAT FORM THE SECOND HOLE.....	15
FIGURE 4.1 THE THREE BLOCK CROSS OVER FOR BIT FLIP MUTATION.....	20
FIGURE 5.1 THE DESIGN DOMAIN OF COMPLIANT DISPLACEMENT AMPLIFIER. ...	22
FIGURE 5.2 THE DESIGN DOMAIN DISCRETIZATION	22
FIGURE 5.3 THE DESIGN DOMAIN SUBDIVISION.....	22
FIGURE 5.4 THE TOPOLOGY OPTIMIZATION RESULTS WITH DOG OF 5 FOR GENERATION 583	24
FIGURE 5.5 THE TOPOLOGY OPTIMIZATION RESULTS WITH DOG OF 5 FOR GENERATION 291	24
FIGURE 5.6 THE GEOMETRIC ADVANTAGE WITH DEGREE OF GENUS 5.	25
FIGURE 5.7 THE VOLUME RATIO, STRESS AND INPUT FORCE WITH DEGREE OF GENUS 5.	25
FIGURE 5.8 THE TOPOLOGY OPTIMIZATION RESULTS WITH DOG OF 6 FOR GENERATION 622.....	26

FIGURE 5.9 THE TOPOLOGY OPTIMIZATION RESULTS WITH DOG OF 6 FOR GENERATION 311	26
FIGURE 5.10 THE GEOMETRIC ADVANTAGE WITH DEGREE OF GENUS 6.	27
FIGURE 5.11 THE VOLUME RATIO, STRESS AND INPUT FORCE WITH DEGREE OF GENUS 6.	28
FIGURE 5.12 THE TOPOLOGY OPTIMIZATION RESULTS WITH DOG OF 7 FOR GENERATION 320.....	28
FIGURE 5.13 THE TOPOLOGY OPTIMIZATION RESULTS WITH DOG OF 7 FOR GENERATION 160.....	29
FIGURE 5.14 THE GEOMETRIC ADVANTAGE WITH DEGREE OF GENUS 7.	29
FIGURE 5.15 THE VOLUME RATIO, STRESS AND INPUT FORCE WITH DEGREE OF GENUS 7.	30
FIGURE 5.16 THE TOPOLOGY OPTIMIZATION RESULTS WITH DOG OF 8 FOR GENERATION 401.....	31
FIGURE 5.17 THE TOPOLOGY OPTIMIZATION RESULTS WITH DOG OF 8 FOR GENERATION 200.....	31
FIGURE 5.18 THE GEOMETRIC ADVANTAGE WITH DEGREE OF GENUS 8.	32
FIGURE 5.19 THE VOLUME RATIO, STRESS AND INPUT FORCE WITH DEGREE OF GENUS 8.	32

FIGURE 6.1 TOPOLOGY WITH DOG 5	34
FIGURE 6.2 MESH FOR TOPOLOGY WITH DOG 5.....	35
FIGURE 6.3 UN-DEFORMED DISPLACEMENT DISTRIBUTION FOR TOPOLOGY WITH DOG 5.....	35
FIGURE 6.4 DEFORMED DISPLACEMENT DISTRIBUTION FOR TOPOLOGY WITH DOG 5.....	36
FIGURE 6.5 UN-DEFORMED STRESS DISTRIBUTION FOR TOPOLOGY WITH DOG 5	37
FIGURE 6.6 DEFORMED STRESS DISTRIBUTION FOR TOPOLOGY WITH DOG 5	37
FIGURE 6.7 THE TOPOLOGY WITH DOG 6.....	38
FIGURE 6.8 MESH FOR THE TOPOLOGY WITH DOG 6.....	39
FIGURE 6.9 UN-DEFORMED DISPLACEMENT DISTRIBUTION FOR TOPOLOGY WITH DOG 6.....	40
FIGURE 6.10 DEFORMED DISPLACEMENT DISTRIBUTION FOR TOPOLOGY WITH DOG 6.....	41
FIGURE 6.11 UN-DEFORMED STRESS DISTRIBUTION FOR TOPOLOGY WITH DOG 6	42
FIGURE 6.12 DEFORMED STRESS DISTRIBUTION FOR TOPOLOGY WITH DOG 6	42
FIGURE 6.13 TOPOLOGY WITH DOG 7	43
FIGURE 6.14 MESH FOR TOPOLOGY WITH DOG 7.....	44

FIGURE 6.15 UN-DEFORMED DISPLACEMENT DISTRIBUTION FOR TOPOLOGY WITH DOG 7	44
FIGURE 6.16 DEFORMED DISPLACEMENT DISTRIBUTION FOR TOPOLOGY WITH DOG 7	44
FIGURE 6.17 UN-DEFORMED STRESS DISTRIBUTION FOR TOPOLOGY WITH DOG 7	46
FIGURE 6.18 DEFORMED STRESS DISTRIBUTION FOR TOPOLOGY WITH DOG 7	47
FIGURE 6.19 TOPOLOGY WITH DOG 8	48
FIGURE 6.20 MESH FOR TOPOLOGY WITH DOG 8.....	49
FIGURE 6.21 UN-DEFORMED DISPLACEMENT DISTRIBUTION FOR TOPOLOGY WITH DOG 8.....	49
FIGURE 6.22 DEFORMED DISPLACEMENT DISTRIBUTION FOR TOPOLOGY WITH DOG 8.....	49
FIGURE 6.23 UN-DEFORMED STRESS DISTRIBUTION FOR TOPOLOGY WITH DOG 8	51
FIGURE 6.24 DEFORMED STRESS DISTRIBUTION FOR TOPOLOGY WITH DOG 8	52
FIGURE 6.25 MESHING FOR THE TOPOLOGY WITHOUT DOG STRATEGY	53
FIGURE 6.26 DISPLACEMENT DISTRIBUTION FOR UN-DEFORMED TOPOLOGY WITHOUT DOG STRATEGY	54

FIGURE 6.27 DISPLACEMENT DISTRIBUTION FOR DEFORMED TOPOLOGY WITHOUT DOG STRATEGY	55
FIGURE 6.28 STRESS DISTRIBUTION FOR UN-DEFORMED TOPOLOGY WITHOUT DOG STRATEGY	55
FIGURE 6.29 STRESS DISTRIBUTION FOR DEFORMED TOPOLOGY WITHOUT DOG STRATEGY	56

LIST OF TABLES

	Page
TABLE 6.1 COMPARISON OF DISPLACEMENT FROM MATLAB AND SOLIDWORKS FOR DOG 5.....	36
TABLE 6.2 COMPARISON OF STRESS FROM MATLAB AND SOLIDWORKS FOR DOG 5.....	38
TABLE 6.3 COMPARISON OF DISPLACEMENT FROM MATLAB AND SOLIDWORKS FOR DOG 6.....	41
TABLE 6.4 COMPARISON OF STRESS FROM MATLAB AND SOLIDWORKS FOR DOG 6.....	43
TABLE 6.5 COMPARISON OF DISPLACEMENT FROM MATLAB AND SOLIDWORKS FOR DOG 7.....	45
TABLE 6.6 COMPARISON OF STRESS FROM MATLAB AND SOLIDWORKS FOR DOG 7.....	47
TABLE 6.7 COMPARISON OF DISPLACEMENT FROM MATLAB AND SOLIDWORKS FOR DOG 8.....	50
TABLE 6.8 COMPARISON OF STRESS FROM MATLAB AND SOLIDWORKS FOR DOG 8.....	52

CHAPTER I

INTRODUCTION

Compliant mechanisms are flexible mechanisms that transfer an input force or displacement to another point through elastic body deformation. The function of a mechanism is to transfer or transform motion, force or energy. A desired function can be realized by a rigid or compliant mechanism. This chapter deals with the introduction of compliant mechanisms, their design criteria, the advantages of compliant mechanisms and the current research situation in the concerned area. A major portion of this work was presented in the publication by Dr. Hong Zhou and Satya R. Kandala [1].

1.1 Topology Optimization of Compliant Mechanisms

The topology optimization of compliant mechanisms is about designing of material layout or distribution. To optimize the topology of a distributed compliant mechanism, its design domain needs to be discretized. For optimizing discrete topology, hexagonal discretization [2], hybrid discretization [3], and modified quadrilateral discretization [4] have been introduced apart from the famous quadrilateral discretization. When compared with gradient-based or continuous topology optimization approaches, discrete topology optimization approach has higher computational costs. However, continuous topology optimization has topology uncertainty problem caused by intermediate material state or grey design cell. In the process of topology optimization using continuous approach, the continuous material density variable has to pass through its middle value (0.5) when the material state represented by the continuous material density is switched from existence to absence or from absence to existence. The problem of topology uncertainty is caused when a material density variable is near 0.5 as its material state is

This thesis report follows the format for the Journal of Mechanical Design, ASME.

neither existent nor absent. When the material state is uncertain, it is also difficult to impose a direct local stress constraint at a point.

In discrete topology optimization, there is no topology uncertainty caused by intermediate material state or grey design cell because binary design variables are used to represent material existence or absence. Topology uncertainty has to be avoided in topology optimization as it leads to different topology solutions and makes topology optimization ambiguous [4]. In any topology solution, high stress concentration, point connection and mesh dependence might cause topology uncertainty and should be removed. Point connection has been eliminated in all of the above three discretization models. The topology solution of a designed compliant mechanism can be different when the same design domain is discretized differently. This thesis is focused on solving this kind of topology uncertainty for discrete topology optimization of distributed compliant mechanisms.

1.2 Criteria for Designing Mechanisms

Topology design of a mechanism plays an important role in the design as it decides the connection relationship of the mechanism and the final performance of the machine. The choice of a suboptimal mechanism in the initial design stages for the machine hinders its performance even if much effort is put into designing in the later detailed design stages of the machine [5]. The overall criteria for designing mechanisms are: high quality, easy maintenance, low cost and environmental friendliness. Following these criteria make machines more competitive on the market and more supportive of environmental sustainability.

To guide the design process of the topology of a rigid mechanism, the degree of freedom (DOF), the number of loops, the number of links, and the number of joints, play a vital role in achieving the topology solution with the solution not being too complicated or away from the

design criteria. Four-bar linkage or its deformation such as crank-rocker linkage is the most popular topology that is widely used because of its simplicity and low cost for its maintenance. It has 1 DOF, 1 loop, 4 links and 4 joints. Simple mechanisms are preferred by designers to maintain low cost. This drives the designers in actively controlling the design processes for rigid mechanisms.

1.3 Advantages of Compliant Mechanisms

A distributed compliant mechanism consists of elastic material and has no joint. The advantage or benefit of compliant mechanisms is that they don't have a joint. Since any point in a compliant mechanism can deform, it is considered to have infinite DOFs in theory. The DOF, the number of links and the number of joints do not exist in compliant mechanisms while compared to the rigid mechanisms. The constraints that are considered for optimizing discrete topology of distributed compliant mechanisms include maximum material volume ratio, stress, input force and input displacement. As the topology solution of compliant mechanisms depends on the number of holes or handles, they cannot be actively controlled by these constraints. The topology solution should be free from the holes after considering all the constraints as it makes the topology complicated and is undesirable for any compliant mechanism. The motivation of this thesis is to introduce a strategy that can control the number of holes and eliminate topology uncertainty from mesh dependence for discrete topology optimization.

1.4 The Degree of Genus

The surface of a compliant mechanism is connected and can be oriented, and its topology is defined by its genus that represents the maximum number of cuttings along non-intersecting closed simple curves without rendering the resultant compliant mechanism disconnected [6]. The genus of a compliant mechanism is its number of holes or handles, the degree of genus (DOG) is

defined in this thesis as the number of holes in a compliant mechanism. The DOG determines the complexity of the compliant mechanism and when constrained in its topology solution, actively controls the complexity. The DOG of a topology is also responsible for eliminating the topology uncertainty from mesh dependency as different discretization lead to topology solutions with the same DOG.

1.5 Current Research Situation

Anupam Saxena has proposed a new honeycomb tessellation and material-mask overlay methods to obtain optimal single-material compliant topologies free from checkerboard and point-flexure pathologies in his thesis “A material-overlay strategy for continuum topology optimization of compliant mechanisms using honeycomb discretization [2].”

Dr. Hong Zhou has introduced the hybrid discretization model for topology optimization of compliant mechanisms in his thesis “Topology optimization of compliant mechanisms using hybrid discretization model [3].” He further continued his work on the hybrid discretization model and introduced modified quadrilateral discretization [4] model for the topology optimization of compliant mechanisms by completely eliminating the point connections.

Zhou, H., Ahmed, N., Uttha, A., have introduced the “Improved Hybrid discretization Model” in which the dangling and redundant solid design cells are removed from topology solutions to promote the material utilization [7].

Chapman, Saitou and Jakiela in their 1994 publication on genetic algorithms explained how the genetic algorithms can be used for optimization problems [10]. They applied the concept of genetic algorithms to a discretized design domain and detailed the mapping methods used in them. They have given so many examples for optimizing the structures using genetic algorithms. They have compared the genetic algorithm techniques with homogenization methods for

optimization. Using their technique, they have generated topologies with high structural performance.

Kane and Schoenaver have addressed structural topology optimization through genetic algorithms in their thesis “Topological optimum design using genetic algorithms [12].” Their approach demonstrates high flexibility, and breaks many limits of standard optimization algorithms.

Wang, N. F, Tai, K., have worked on producing symmetric paths using compliant mechanisms [16].

The present thesis work has focused on introducing a new strategy in order to eliminate Topology Uncertainty in compliant mechanisms.

1.6 Research, Motivation and Approach

The motivation of this thesis, The Uncertainty Elimination in Discrete Topology Optimization of Compliant Mechanisms, is to eliminate the Topology Uncertainty problem that usually exists in most of the Topology Optimization problems.

The thesis implements the hybrid discretization model to the discrete topology optimization of compliant mechanisms. Dangling and redundant quadrilateral design cells result in undesirable sharp protrusions. The DOG Control strategy is introduced in this thesis to address the problem of mesh dependence. The number of holes in an optimized topology is actively controlled in this process. The obtained topology is free from redundant and dangling cells, point connections and is independent of the employed mesh. The von Mises stress is calculated for each triangular analysis cell and a direct stress constraint is imposed on it to make the obtained optimal topology safe. A bit-array representation based GA is used to search for the optimal topology.

The topology solutions are independent of the employed meshes. The mesh dependence problem in the discrete topology optimization is eliminated.

1.7 Thesis Organization

The current thesis is organized into six chapters. The details included in each chapter are discussed below.

The first chapter includes the introduction of compliant mechanisms, topology optimization, criteria for optimization, advantages of compliant mechanisms, defining the Degree of Genus, current research situation, motivation and the thesis organization.

The Degree of Genus control strategy is discussed in detail in the Chapter 2 of this thesis.

The Chapter 3 deals with the topology optimization formulation.

The Chapter 4 introduces the optimization algorithm and the implementation of the algorithm in discrete topology optimization.

The Chapter 5 demonstrates the use of the Degree of Genus Control Strategy for Compliant displacement amplifier considering different DOGs and comparing the respective constraints like maximum material volume ratio, stress, input force and input displacement.

In chapter 6, the results obtained from MATLAB are validated against the results obtained from SolidWorks.

In Chapter 7, the results, conclusions and the future scope of the current thesis work is discussed.

CHAPTER II

THE DOG CONTROL STRATEGY

The number of holes or handles in a compliant mechanism defines the DOG of the mechanism. The motive of the DOG control strategy in the process of optimizing the discrete topology is to constrain the DOG of a designed compliant mechanism. The hybrid discretization model and the DOG computation guide the DOG control strategy and are explained in this chapter.

2.1 Discretization of the Design Domain

Hybrid discretization has more local topology search directions [3] when compared to other discretization and hence is used in the thesis. In the hybrid discretization model, the entire design domain is discretized into quadrilaterals and each quadrilateral is further subdivided into triangles. Quadrilaterals are used as design cells and triangles for finite element analysis. The Figure 2.1 shows a subdivided quadrilateral design cell in which the four inner triangles are marked by "I" while the four corner triangles by "C". Two neighboring quadrilateral design cells share four corner triangles as shown in Figure 2.2 in horizontal, vertical and diagonal situations.

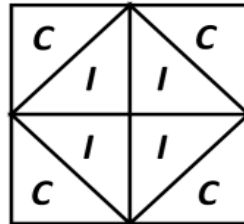


Figure 2.1 A subdivided quadrilateral design cell with its inner and corner design cells

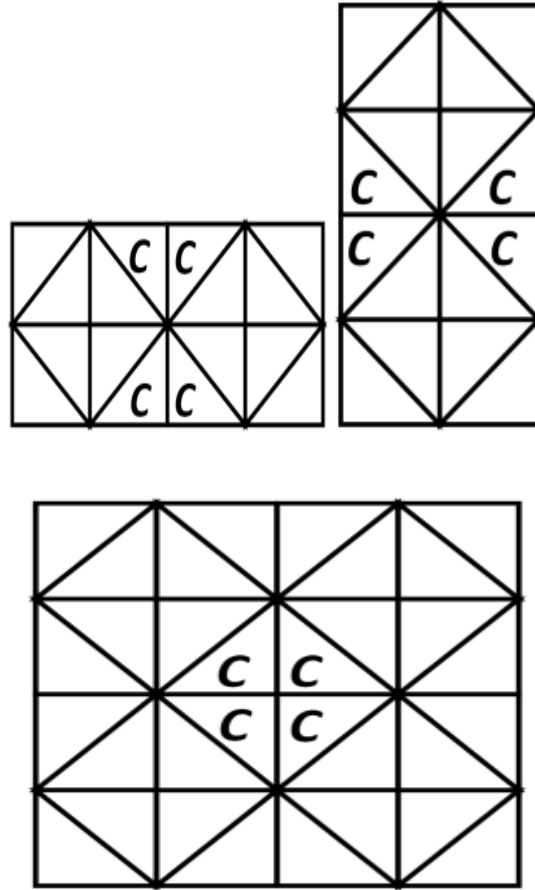


Figure 2.2 The four corner triangles between two neighboring quadrilateral design cells

In a topology solution, each quadrilateral design cell is considered to have a binary material state which is either a solid or a void. In a quadrilateral design cell, the four inner triangles directly represent the material state of the quadrilateral design cell while the four corner triangles have the material state depending on the quadrilateral design cell itself and its neighboring quadrilaterals. The four corner triangles between two neighboring quadrilateral design cells are solid only when both of the two neighboring quadrilateral design cells are solid. Two solid neighboring quadrilateral design cells in different directions are shown in Figure 2.3.

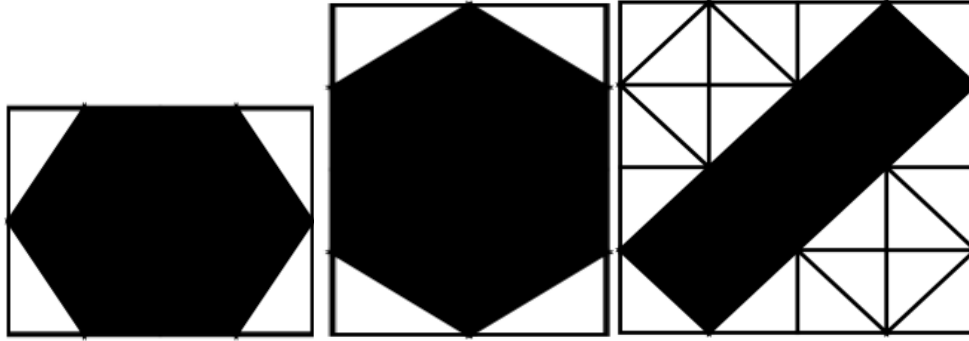


Figure 2.3 Two solid neighboring quadrilateral design cells in different directions

2.2 Computing the DOG

2.2.1 Discretizing the design domain

A cantilever beam is considered to explain the DOG computation for the discrete topology optimization. The Figure 2.4 shows the quadrilateral discretization of the cantilever beam into quadrilateral design cells which is subdivided into triangular analysis cells using the hybrid discretization model. The external load is considered to be exerting at the bottom right corner of the design domain.

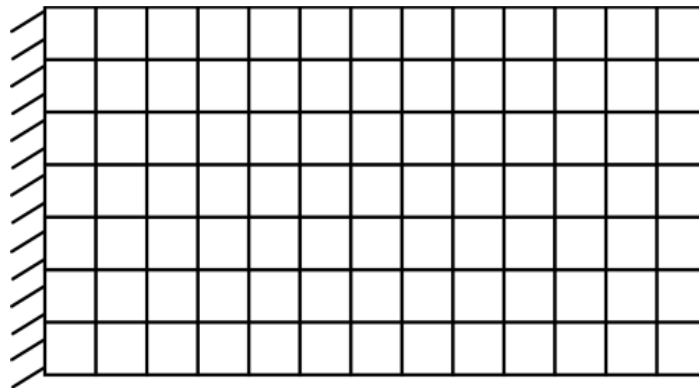


Figure 2.4 The quadrilateral design cells in hybrid discretization model.

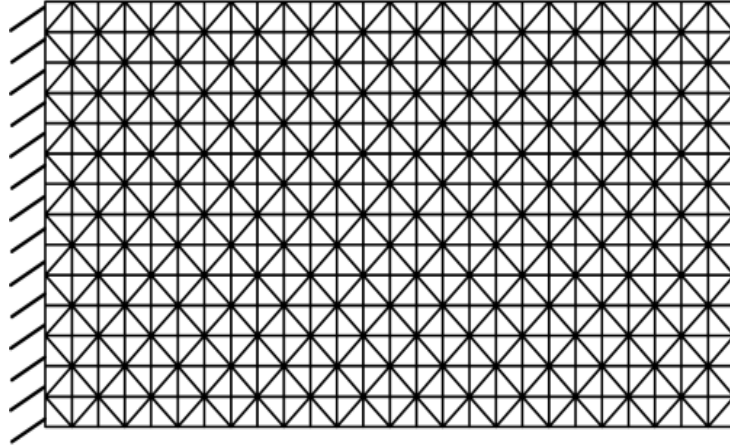


Figure 2.5 The subdivided triangular analysis cells in hybrid discretization model.

2.2.2 Removal of dangling and redundant Cells

The topology of the cantilever beam with some dangling and redundant cells in the discretized and subdivided design domain has been shown in Figure 2.5. A dangling design cell is a solid design cell that is only connected to one neighboring solid design cell and a redundant design cell can be an adjacent upper, lower, left or right design cell [7]. An upper redundant design cell is a solid design cell which has its left, right and three upper contiguous design cells as void. Lower, left and right redundant design cells can similarly be defined.

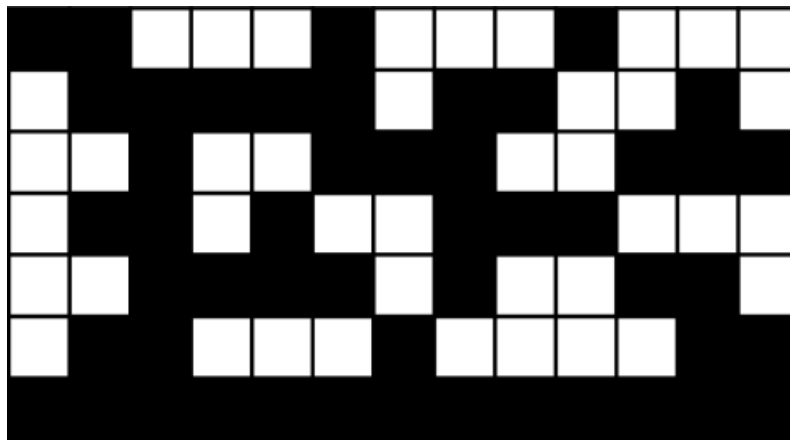


Figure 2.6 The quadrilateral design cells of a topology

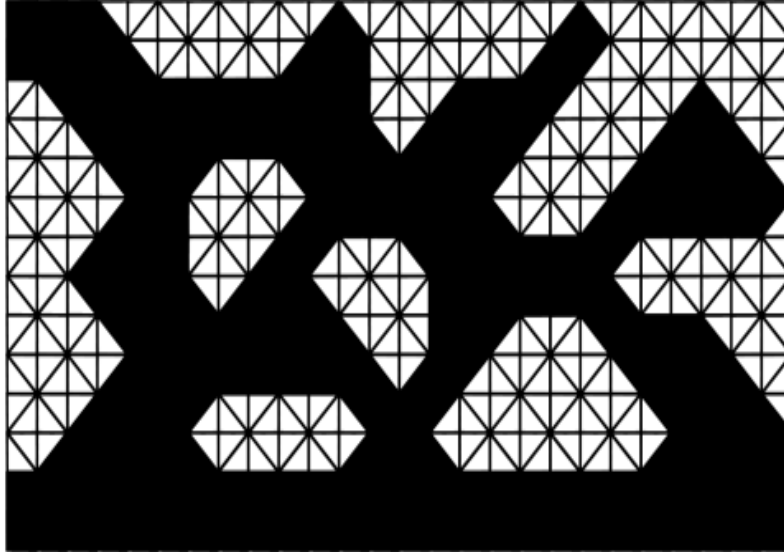


Figure 2.7 The triangular analysis cells of a topology

The modified topology of Figure 2.5 after the removal of the dangling and redundant cells is shown in Figure 2.6. Topology remains the same in the process of removing dangling and redundant design cells.

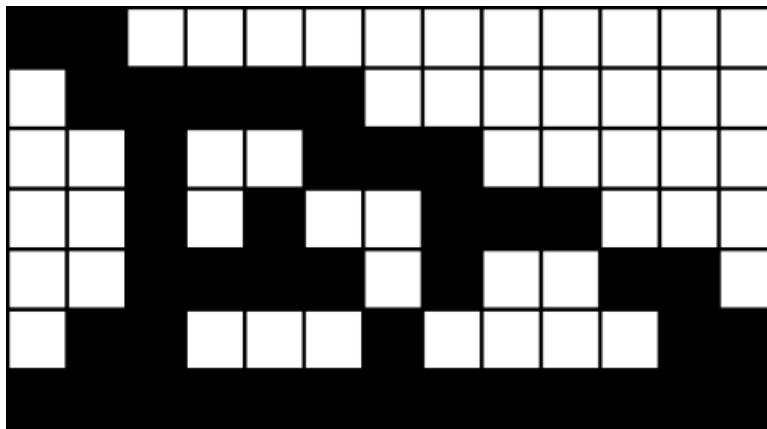


Figure 2.8 The Topology of Figure 2.5 after removing dangling and redundant design cells.

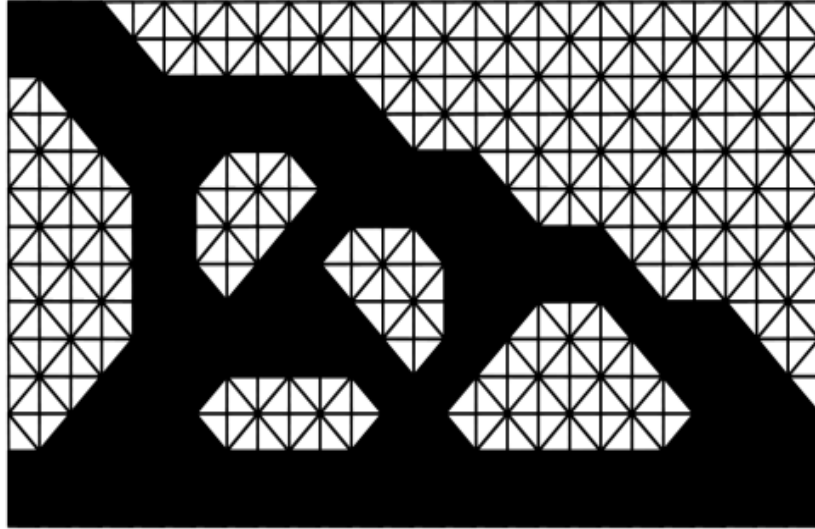


Figure 2.9 The Topology of Figure 2.5 after removing dangling and redundant design cells.

2.2.3 Flipping the design cells

As shown in Figure 2.6, in a hybrid discretization model, two void neighboring design cells are connected only if they are in the horizontal or vertical direction and cannot be connected if they are diagonally neighboring each other. For calculating the number of holes in a topology, the topology needs to be considered from the discretized design domain. For the purpose of calculation of the number of holes in a topology, the design cells are required to be flipped which makes the solid design cells void and the void design cells solid as shown in Figure 2.7.

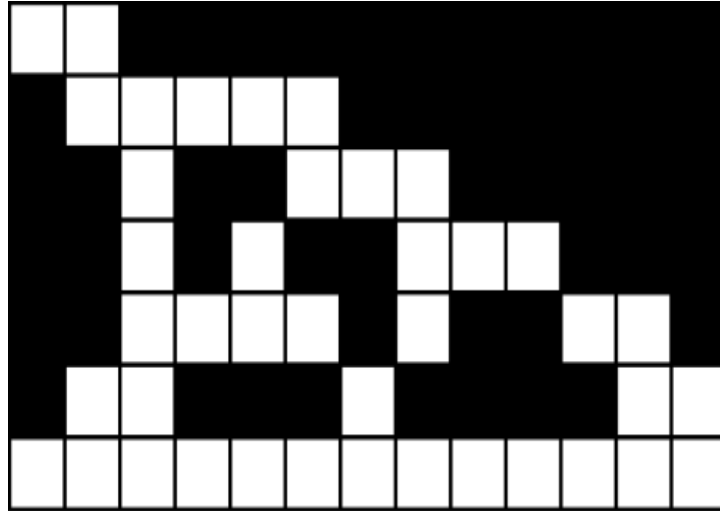


Figure 2.10 The flipped topology of Figure 2.6 in the discretized design domain

Once the topology is flipped, its binary adjacency matrix can be established. The binary connectivity matrix of the flipped topology can then be derived from its binary adjacency matrix [8]. The void design cells on the boundary of the initial topology are responsible for the formation of holes. To remove these holes from the original topology, the solid design cells in the flipped topology are needed to be removed if they are connected to any solid design cells in the boundary. The topology after removing the solid design cells in the flipped topology is shown in Figure 2.8.

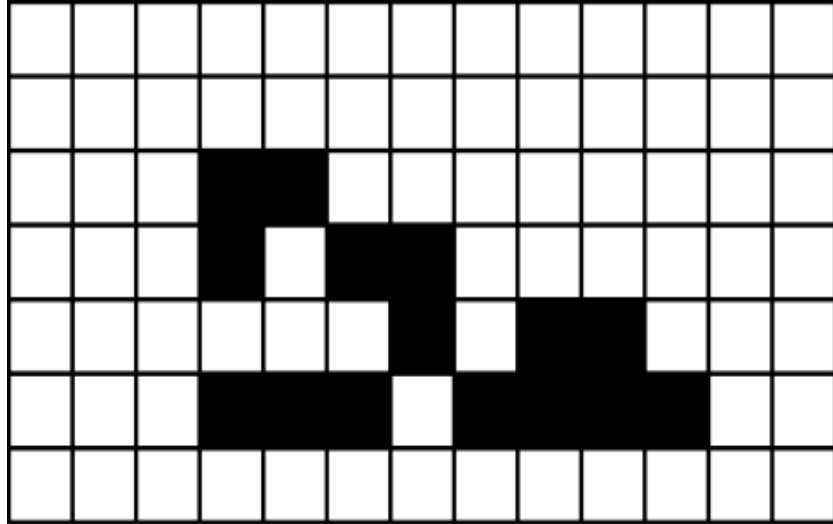


Figure 2.11 The topology of Figure 2.7 after removing solid design cells that are connected to any solid boundary design cell

2.2.4 Counting the Number of holes in the Topology

The solid design cells in Figure 2.8 are responsible for the formation of holes in the topology. All the design cells in the Figure 2.8 are scanned from left to right and from top to bottom for the purpose of counting the number of holes in the topology. In the process of counting, when a solid design cell is found, the hole counter is increased to one, the solid design cell itself and the adjacent solid design cells connecting it are flipped to void. Figure 2.9 shows the yielded topology of Figure 2.8 after the removal of the first hole.

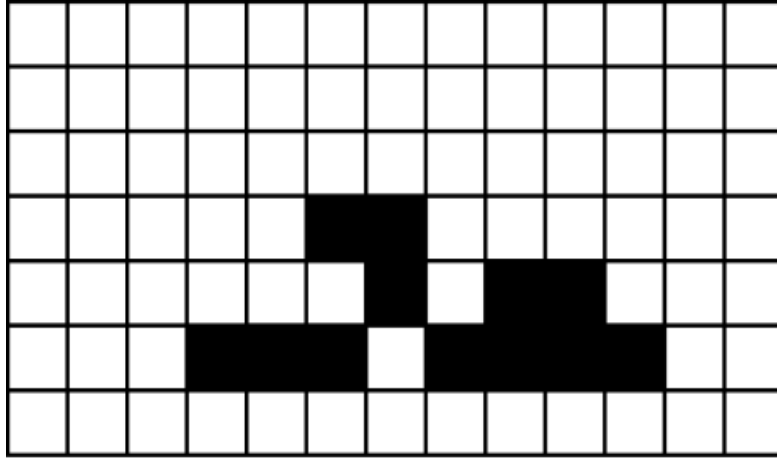


Figure 2.12 The topology after removing the solid design cells forming the first hole

When the similar process is applied to the existing solid design cells in Figure 2.9, the resultant topology is shown in Figure 2.10 after the removal of second hole.

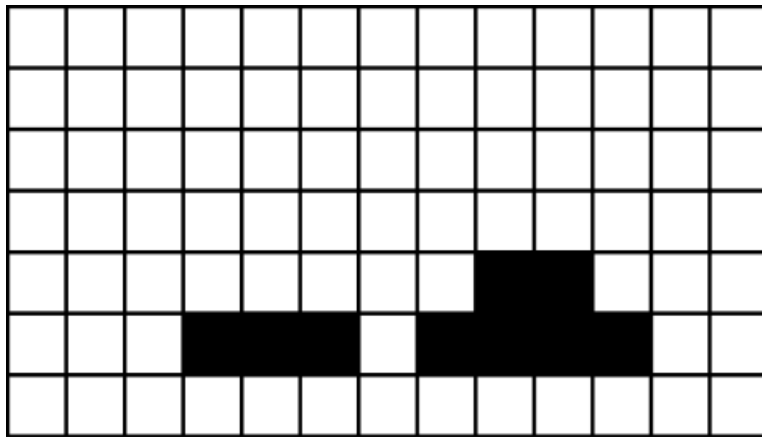


Figure 2.13 The Topology after removing the solid design cells that form the second hole

The total number of holes of Figure 2.8 can be obtained after all design cells are scanned, which is 4 for this topology

CHAPTER III

TOPOLOGY OPTIMIZATION FORMULATION

The general formulation for topology optimization can be stated as follows.

$$\text{Maximize } \varphi(X) \quad (1)$$

$$\text{Subject to } \{g_j(X) \leq 0, j= 1, 2, \dots, \eta\} \quad (2)$$

Here X specifies the values of all design variables. $\varphi(X)$ is the problem-dependent objective to be maximized, $g_j(X)$ is the set of constraints and η is the total number of constraints. All design variables are binary and take either 1 or 0 value in the proposed topology optimization method. They can be represented as a binary array when the design domain is discretized into certain numbers of rows and columns of quadrilaterals. We then have $x = [x_{ij}]$, $i = 1, 2, \dots, m$, $j=1,2,\dots,n$. Here m and n are the numbers of rows and columns of quadrilateral design cells in the discretization, respectively.

The mechanical advantage and the material utilization are the key attributes which constrain the topology optimization. In the introduced approach for optimizing the topology, the degree of genus is a major constraint using which the number of holes in a topology is actively controlled. It is desired that high stiffness is realized by using less material [9]. The reciprocal of the compliance $c(x)$ of a mechanism defines the stiffness of the mechanism. Compliance can be calculated as $c(X) = F^T U$. F and U are the global force and displacement vectors, respectively. F and U meet the global equilibrium equation. $KU = F$. Here K is the global stiffness matrix. Thus, the optimization formulation can be written as

$$\text{Maximize } \varphi(X) = 1/c(X) \quad (3)$$

$$\text{Subject to } g_1(X) = v(X)/v_0 - r_v \leq 0 \quad (4)$$

$$g_2(X) = \text{Max}\{\sigma_j/\sigma_a\} - 1 \leq 0, j = 1,2, \dots, N \quad (5)$$

v and v_0 are the actual material volume and the design domain volume, respectively. r_v is the allowed volume ratio, σ_j and σ_a are the von Mises stress of analysis cell j and the allowed von Mises stress, respectively. The von Mises stress at the centroid of an analysis cell is used as a criterion in determining the onset of failure of the analysis cells. N is the total number of triangular analysis cells in the design domain, which is equal to $8*m*n$.

In the discrete topology optimization, fine discretization not only increases the number of design variables, but also introduces small holes to the topology solutions. Coarse discretization usually decreases the analysis precision. With the design cell subdivision, a fine mesh can be realized with a moderate number of design variables since mesh fineness depends on the number of analysis triangles and the number of design variables equals the number of quadrilaterals.

CHAPTER IV

OPTIMIZATION ALGORITHM

The optimal topology of different structures can be found using Genetic algorithms (GAs) search criteria [10-11]. In GA based optimizations, Topologies have been represented by binary bit strings which have been widely used in different applications because of their easy implementations. However, in discrete topology optimization, it was found that binary bit-string representation is geometrically biased against the vertical design cells [12]. In the bit string representation, the adjacent bits may not correspond to the neighboring vertical design cells in a discretized design domain and are far away from each other which results in geometric bias because one-point or multi-point crossovers can only exchange the horizontal bands of the parents. This drawback is restricted in the binary bit-array representations as the binary bit array representations do not have the geometric bias drawback since tile adjacency relationship of design cells in binary bit array representation is exactly the same as that in the design domain [12-14]. The GA based discrete topology optimization also uses the morphological representation apart from the bit-array representation for discrete topology optimization [15-17]. Binary bit-arrays have been used for all the topologies used in this thesis.

The design cells used for the loading and supporting the mechanism are required to be solid and connected for topologies to be valid. In the process of optimization of topologies, disconnected topologies are generated which are invalid but provide useful information for crossover operation and maintaining diversities for the pool of individual solutions. The disconnected topologies are disregarded and the connected topologies are considered for the process of optimization.

4.1 Criteria for Finding Connectivity of Design Cells

The connectivity matrix determines the connectivity relationship of any topology which is indeed derived from the adjacency matrix of the topology [8]. These two matrices are binary matrices of $M \times M$ order where M is the total number of design cells in the design domain, which is $M = m \times n$. The connectivity matrix, being symmetric, exactly represents any loading or supporting design cells in which the rows and columns represent the respective design cells. From the connectivity matrix, it can be determined if a particular design cell is connected or not from the corresponding row or column. A topology is considered to be connected or disconnected if the special design cells such as loading or supporting design cells are connected or disconnected respectively.

4.2 Generation of Pool for Selecting Optimum Topology

A connected topology is evaluated for its objective and constraint functions and when a constraint is violated, the topology is penalized while calculating its fitness. The initial pool of all topologies is randomly produced and then a mating pool is generated by combining the tournament selection and elitist selection. Tournament selection restricts the overly fit topologies from dominating the selection process [18] while the elitist selection strategy concentrates on pushing the fittest topology to the next generation.

In this thesis, Block crossover [12-13] is employed in which the binary bit-arrays of two parents are cut into nine blocks by two horizontal lines and two vertical lines. The process of bit flip mutation is employed after randomly selecting three blocks of the two parents and exchanged as shown in the figure. This process is continued for certain number of generations until the best fitness value does not change.

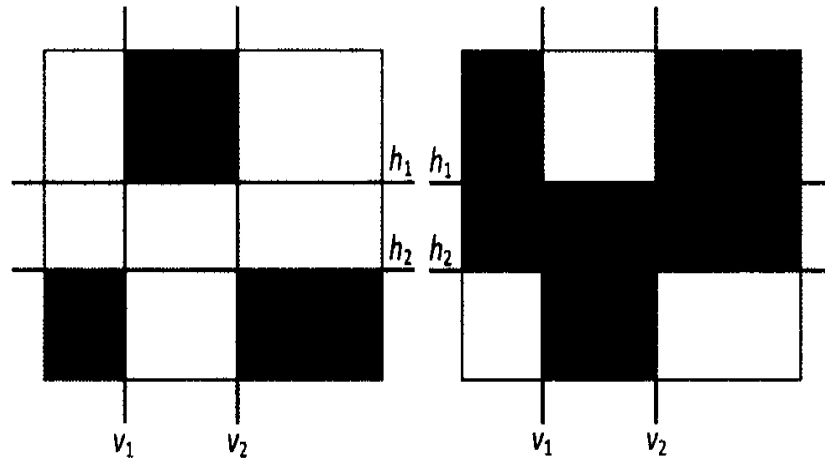


Figure 4.1 The three block cross over for bit flip mutation.

CHAPTER V

TOPOLOGY OPTIMIZATION EXAMPLES

The purpose of introducing the DOG control strategy in this thesis is to ease the process of controlling the topology optimization of compliant mechanisms. To meet the aesthetic demands or any practical requirements, the DOG of a designed compliant mechanism can be constrained to a specific number or a certain range so that the topology solution has minimum complicacy like having less number of holes. A compliant displacement amplifier is considered as an example to demonstrate the DOG control strategy for the topology optimization by using distinct values of DOGs.

5.1 Compliant Displacement Amplifier

In this topology optimization example, the direction of the output displacement is required to be opposite to the input displacement and the magnitude of the output displacement needs to be amplified under a certain input displacement. The design domain size is 100 mm x 100 mm with the out-of-plane thickness of 2mm. The material of the compliant mechanism is polycarbonate with the Young's modulus (E) of 2000 N/mm², the Poisson's ratio (ν) of 0.37, the allowed stress (σ_a) of 60 N/mm². The design domain, its discretization and subdivision are shown in Figures 5.1 to 5.3 respectively. The spring stiffness at the output port is taken as $k_{out} = 2$ N/mm. The entire design domain is discretized into 5 mm x 5 mm (14pg) square design cells. There are 20 design cells in the vertical direction and 20 design cells in the horizontal direction. Each design cell is subdivided into 8 triangular analysis cells, so there are totally 3200 triangular analysis elements. Since the upper half of the design domain is symmetric to the lower half, only the upper half needs to be analyzed and designed. We thus have $m = 10$ and $n = 20$. The bit-array representation for any topology is a binary 10 x 20 matrix.

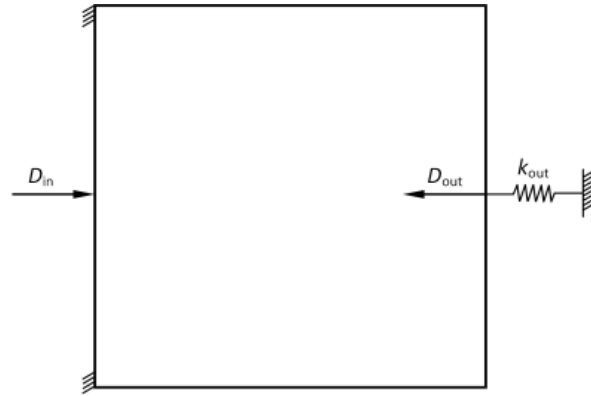


Figure 5.1 The design domain of compliant displacement Amplifier.

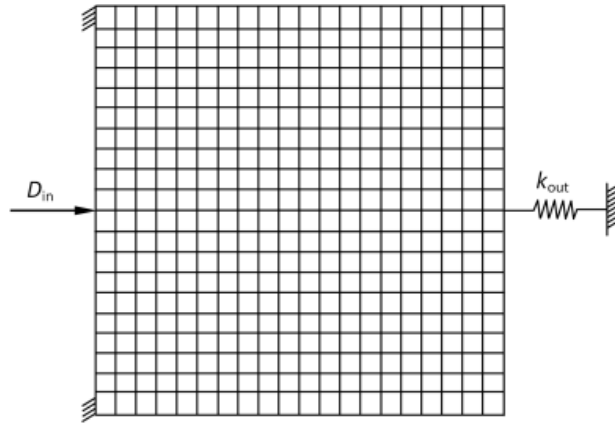


Figure 5.2 The design domain discretization

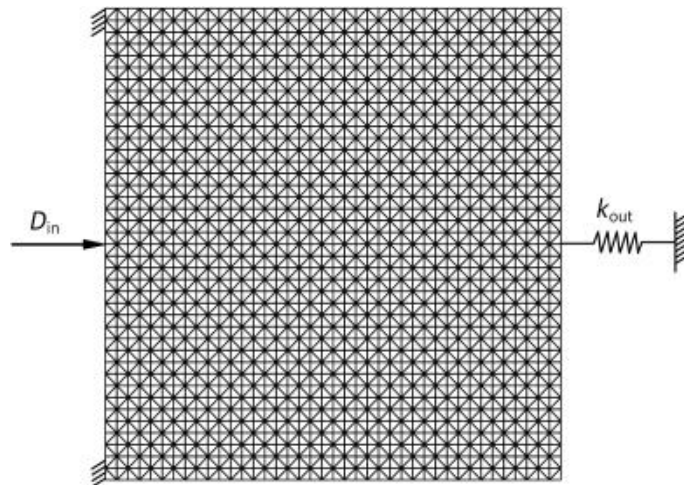


Figure 5.3 The design domain subdivision.

The function of the compliant mechanism is to invert and amplify the input displacement. So the objective of topology optimization can be considered as maximizing the geometric advantage of the synthesized compliant mechanism and defined as follows.

$$\varphi(\mathbf{X}) = \text{sign}(D_{out}) |D_{out} / D_{in}| \quad (6)$$

Here D_{out} and D_{in} are the generated output and the specified input displacements, respectively. D_{in} is specified as 2 mm, $\text{sign}(D_{out})$ defines a certain direction of D_{out} as positive, and its opposite direction as negative.

The von Mises stress of every analysis cell can be calculated from the finite element analysis. The maximum von Mises stress of all analysis cells needs to be below its allowed value of the material. The input force required to generate the specified input displacement is also under a certain restriction. The inequality constraints in this example include the material volume constraint, local stress constraint and input force constraint. These constraints can be defined as follows,

$$g_1(\mathbf{X}) = v(\mathbf{X}) / v_0 - r_v \leq 0 \quad (7)$$

$$g_2(\mathbf{X}) = \text{Max}\{\sigma_j / \sigma_a\} - 1 \leq 0, j = 1, 2, \dots, N \quad (8)$$

$$g_3(\mathbf{X}) = F_{in} / F_a - 1 \leq 0 \quad (9)$$

F_{in} and F_a are the actual maximum input force and the allowed maximum input force, respectively. When the DOG of the compliant mechanism is set at a specific number, the following constraint can be added.

$$g_4(\mathbf{X}) = H(\mathbf{X}) - R_D = 0 \quad (10)$$

$H(\mathbf{X})$ is the number of holes in the topology candidate. R_D is the required DOG for the compliant mechanism.

5.1.1 The topology optimization results with DOG of 5

In this example, r_v and F_α are 0.3 and 100 N. The crossover and mutation probabilities are 0.85 and 0.01. The population size is 150. The tournament and elitist selection parameters are 4 and 2, respectively. The stopping criterion is 100 generations in which the best fitness does not change. When R_D is set as 5, the topology optimization results are shown in Figure 5.4.

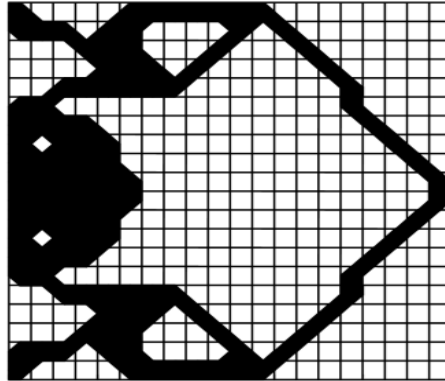


Figure 5.4 The Topology optimization results with DOG of 5 for Generation 583

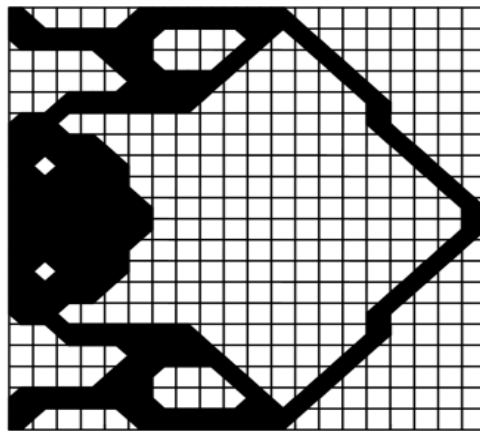


Figure 5.5 The Topology optimization results with DOG of 5 for Generation 291

At generation 583, the output displacement and the geometric advantage are 4.24 mm and 2.12, respectively. Its actual volume ratio is 0.30. The required input force is 99.23 N to generate the specified input displacement of 2 mm. The maximum von Mises stress of all analysis cells is

50.68 N/mm². The best fitness does not change from generation 484, to generation 583, so the search stops at generation 583. The geometric advantage at generations 291 is 2.11, which is very close to the optimal topology. Figure 5.5 Shows the geometric advantage of the individual with the best fitness at each generation. The volume ratio, the maximum von Mises stress and the input force of the best individual at each generation are shown in figure 6.6.

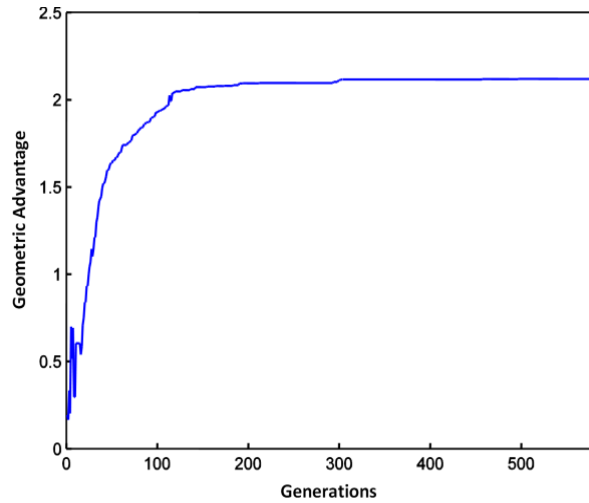


Figure 5.6 The Geometric Advantage with Degree of Genus 5.

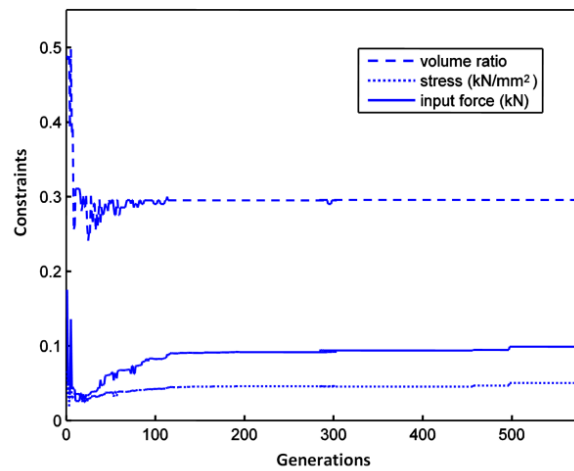


Figure 5.7 The Volume Ratio, stress and Input force with Degree of Genus 5.

5.1.2 The topology optimization results with DOG of 6

When R_D is set as 6, the topology optimization results are shown in Figures 5.8 and 5.9.

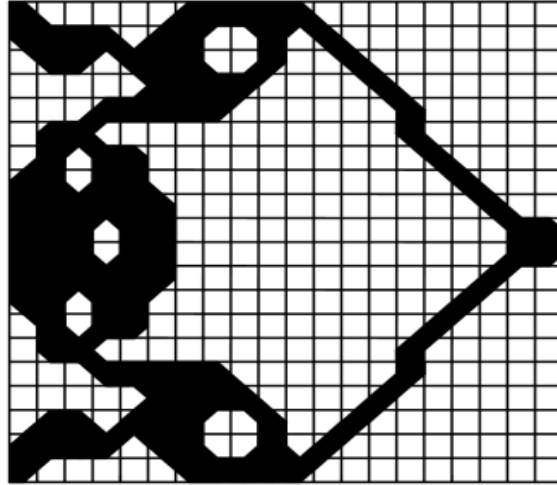


Figure 5.8 The Topology optimization results with DOG of 6 for Generation 622

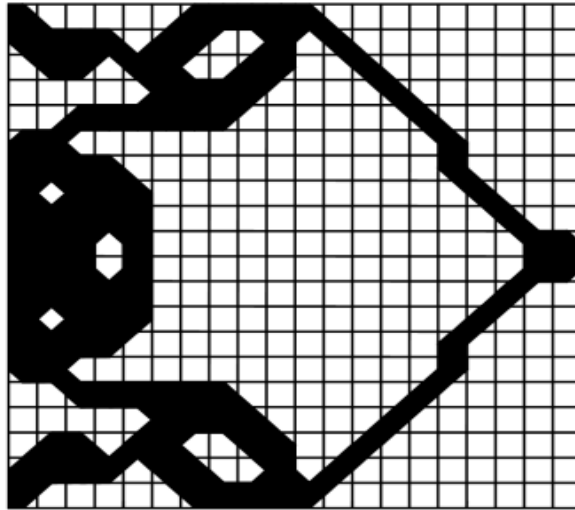


Figure 5.9 The Topology optimization results with DOG of 6 for Generation 311

At generation 622 the output displacement and the geometric advantage are 3.98 mm and

1.99, respectively. Its actual volume ratio is 0.30. The required input force is 94.80 N to generate the specified input displacement of 2mm. The maximum von Mises stress of all analysis cells is 53.83 N/mm². The best fitness does not change from generation 523 to generation 622, so the search stops at generation 622. The geometric advantage at generations 311 is 1.95, which is close to the optimal topology. Figure 5.8 shows the geometric advantage of the individual with the best fitness at each generation. The volume ratio, the maximum von Mises stress and the input force of the best individual at each generation are shown in Figure 5.9.

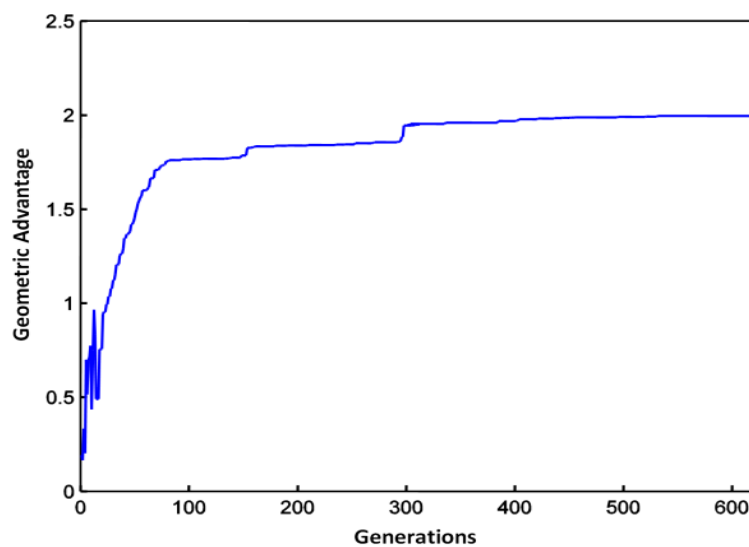


Figure 5.10 The Geometric Advantage with Degree of Genus 6.

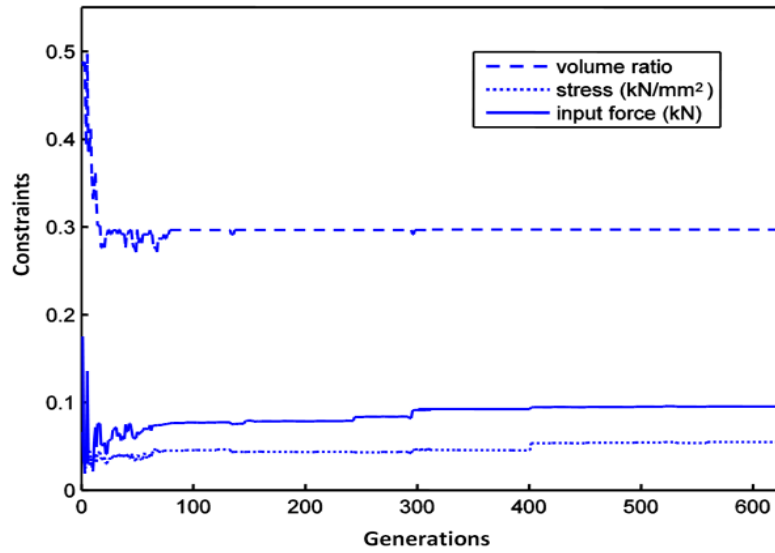


Figure 5.11 The Volume Ratio, stress and Input force with Degree of Genus 6.

5.1.3 The topology optimization results with DOG of 7

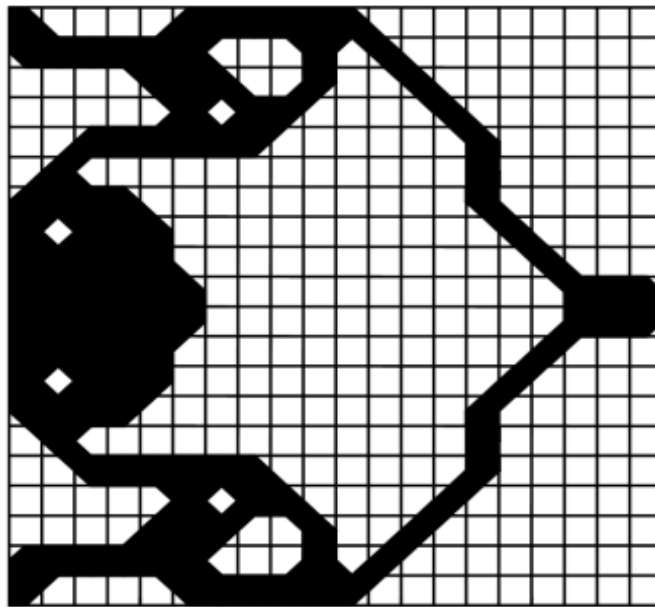


Figure 5.12 The Topology optimization results with DOG of 7 for Generation 320.

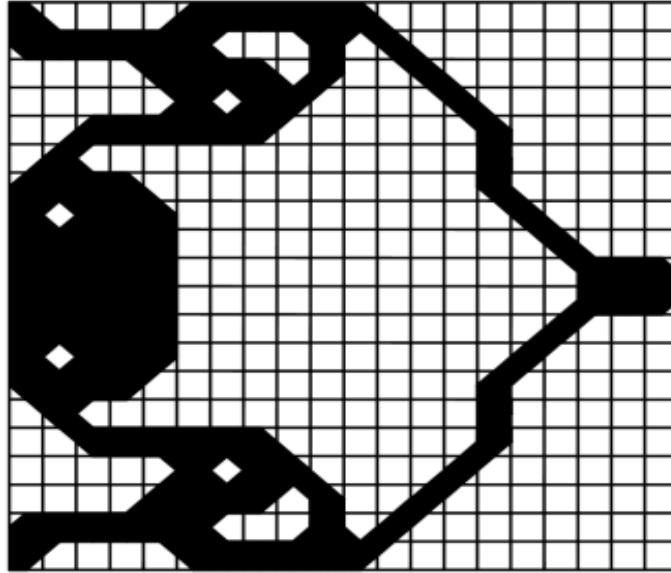


Figure 5.13 The Topology optimization results with DOG of 7 for Generation 160.

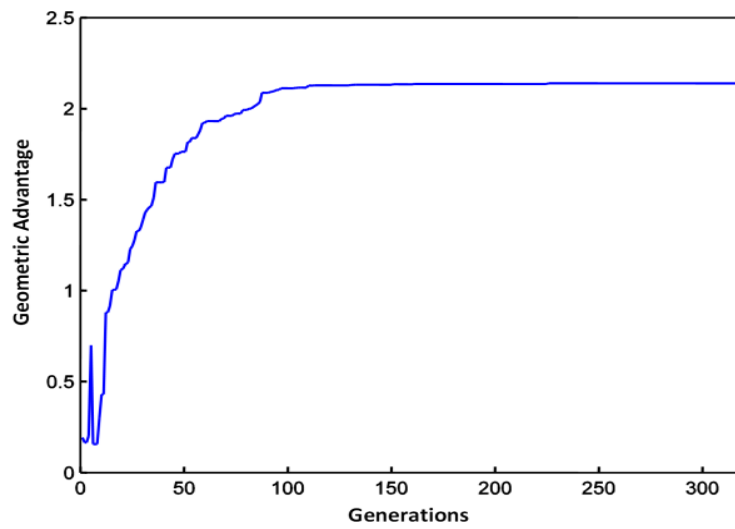


Figure 5.14 The Geometric Advantage with Degree of Genus 7.

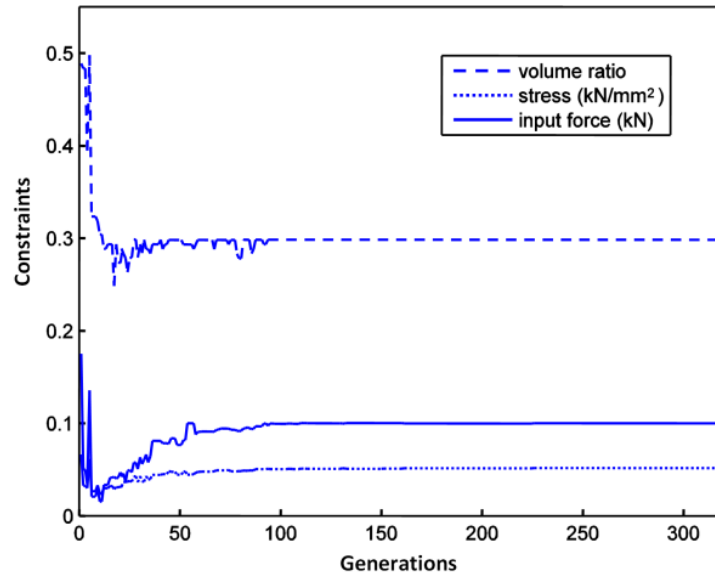


Figure 5.15 The Volume Ratio, stress and Input force with Degree of Genus 7.

When DOG is 7, the output displacement and the geometric advantage of the optimal topology are 4.26 mm and 2.13 respectively. Its actual volume ratio is 0.30. The required input force is 99.69 N to generate the specified input displacement of 2 mm, The maximum von Mises stress of all analysis cells is 51.35 N/mm².

5.1.4 The topology optimization results with DOG of 8

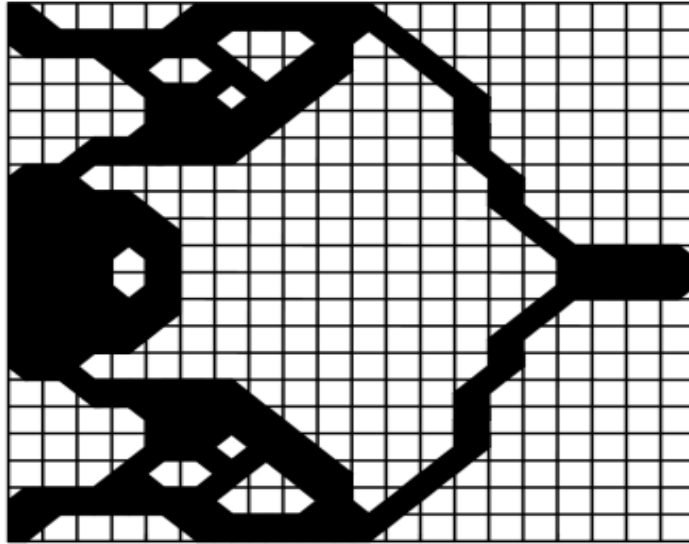


Figure 5.16 The Topology optimization results with DOG of 8 for Generation 401.

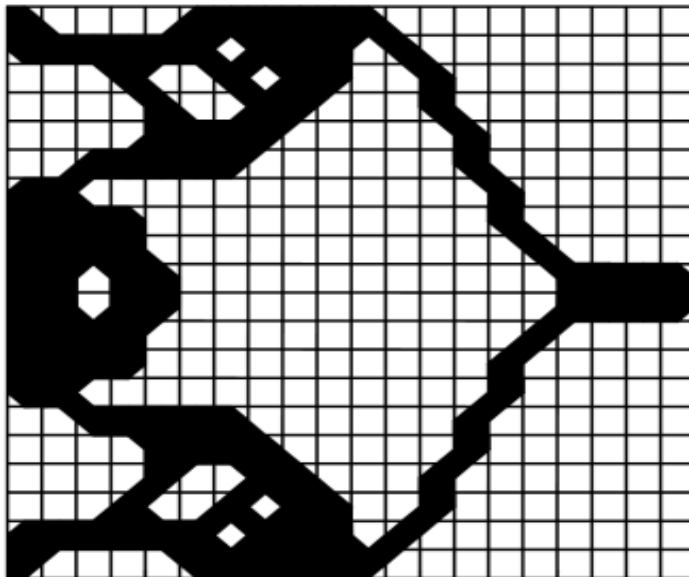


Figure 5.17 The Topology optimization results with DOG of 8 for Generation 200.

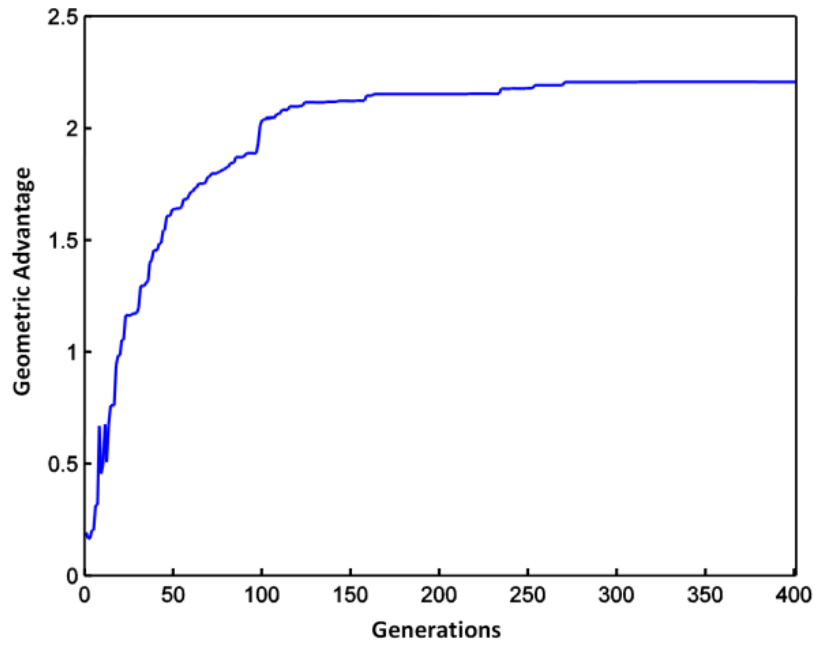


Figure 5.18 The Geometric Advantage with Degree of Genus 8.

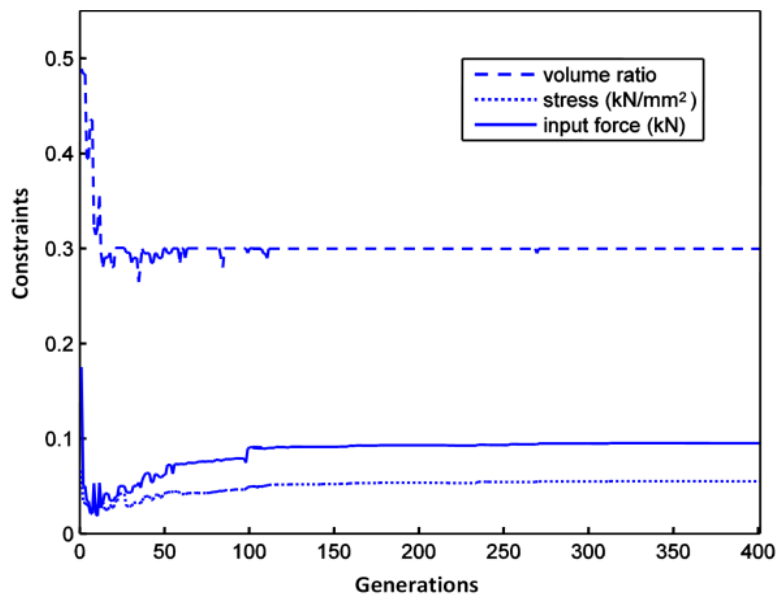


Figure 5.19 The Volume Ratio, Stress and Input Force with Degree of Genus 8.

When DOG is 8, the output displacement and the geometric advantage of the optimal topology are 4.42 mm and 2.21, respectively. Its actual volume ratio is 0.30. The required input force is 95.33 N to generate the specified input displacement of 2 mm. The maximum von Mises stress of all analysis cells is 54.60 N/mm².

CHAPTER VI

RESULTS FROM SOLID WORKS

The results obtained from the Matlab are validated with the ones from SolidWorks for each topology. This chapter discusses them in detail for all the topologies used in this thesis.

6.1 Results for DOG 5

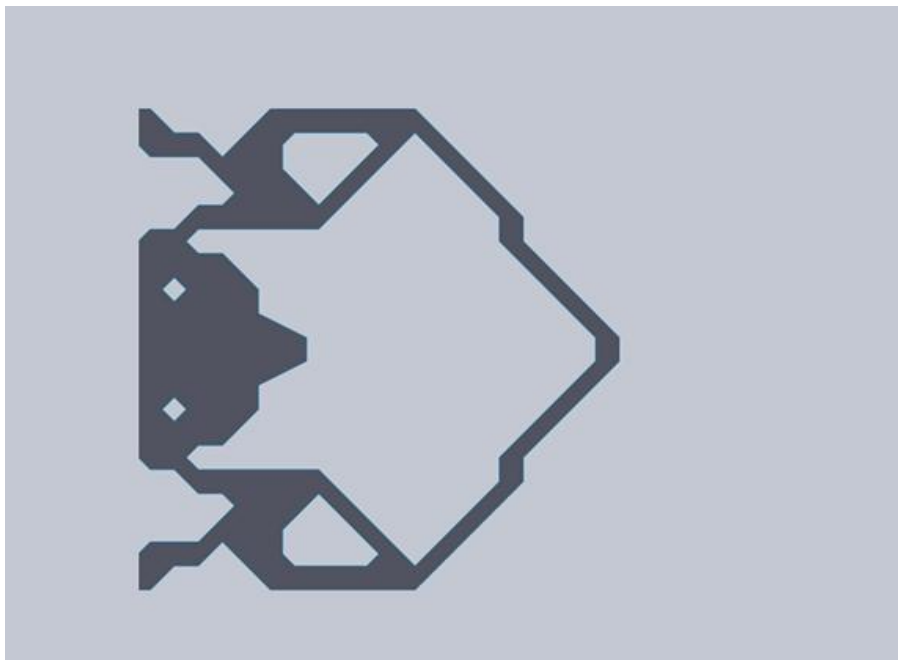


Figure 6.1 Topology with DOG 5

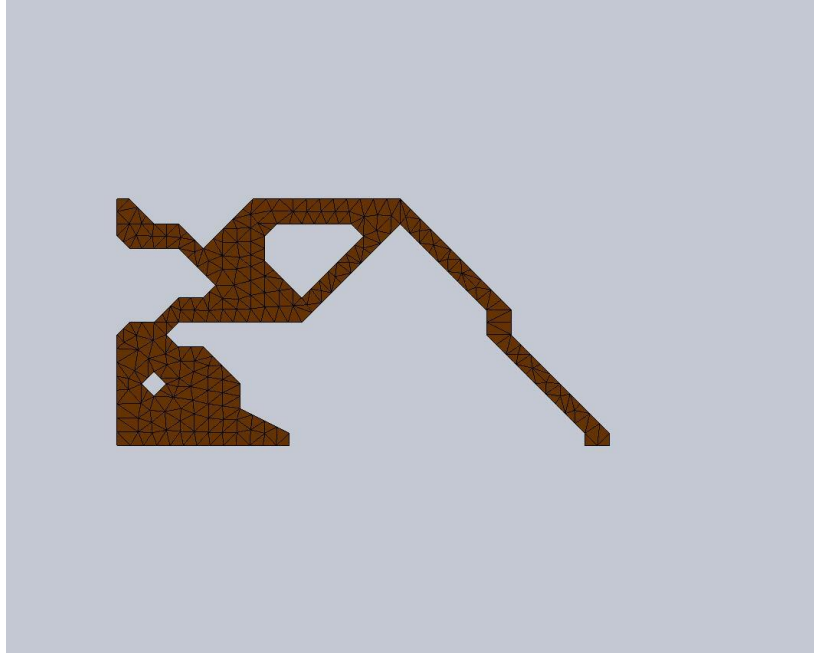


Figure 6.2 Mesh for topology with DOG 5

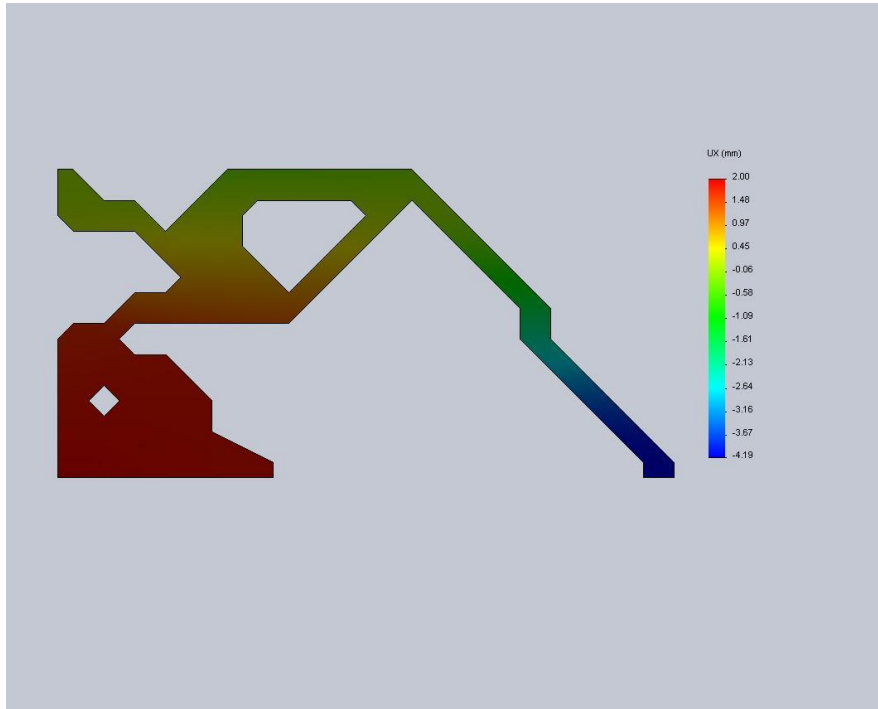


Figure 6.3 Un-deformed Displacement Distribution for topology with DOG 5

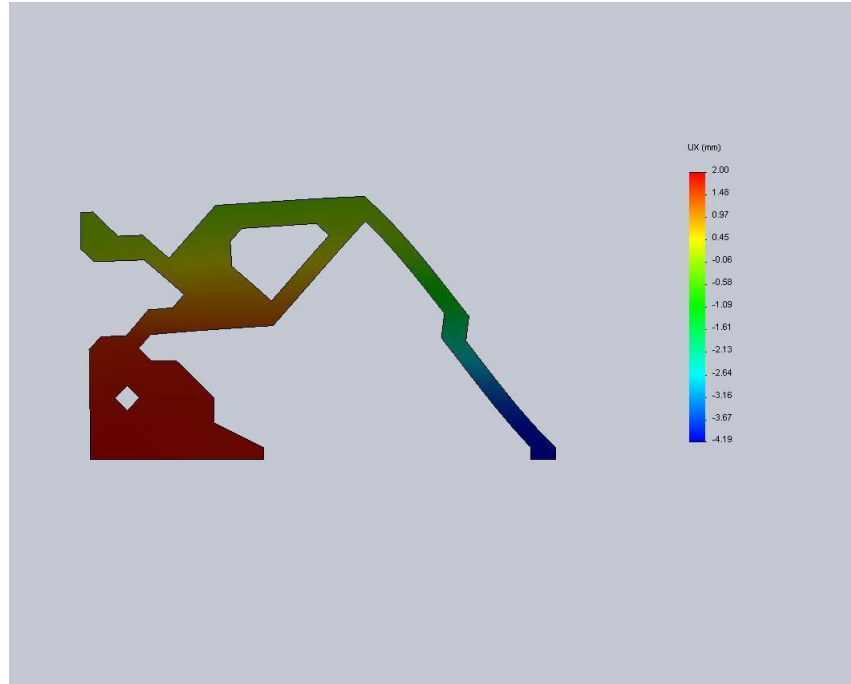


Figure 6.4 Deformed Displacement Distribution for topology with DOG 5

Table 6.1 Comparison of displacement from MATLAB and SolidWorks for DOG 5

DOG	MATLAB	SOLIDWORKS	Difference %
	Displacement	Displacement	
	(mm)	(mm)	
5	4.24	4.19	-1.15

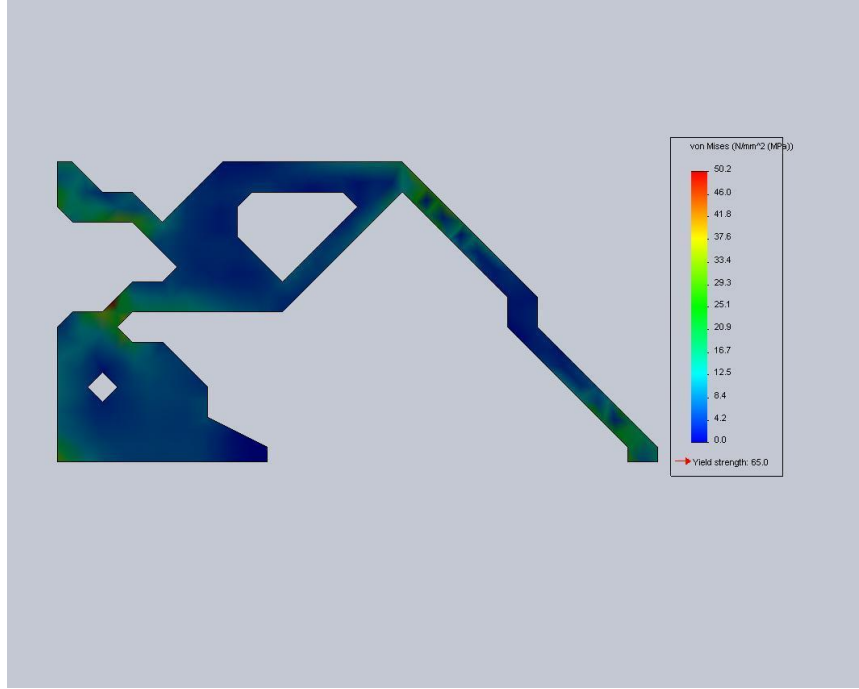


Figure 6.5 Un-deformed Stress Distribution for topology with DOG 5

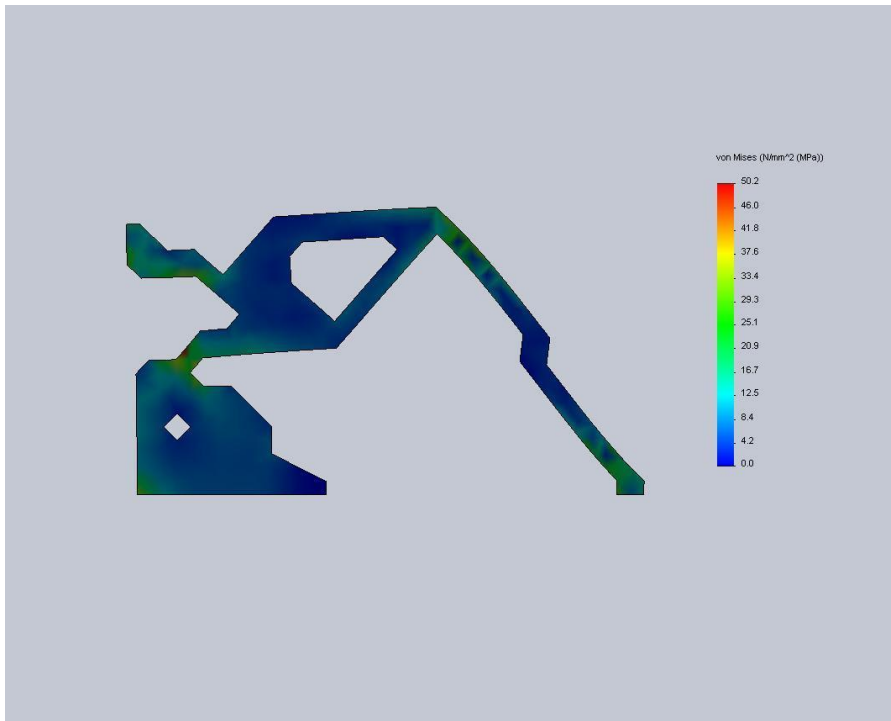


Figure 6.6 Deformed Stress Distribution for topology with DOG 5

Table 6.2 Comparison of stresses from MATLAB and SolidWorks for DOG 5

DOG	MATLAB	SOLIDWORKS	Difference %
	Stress (N/mm ²)	Stress (N/mm ²) ²	
5	50.68	50.2	-0.94

6.2 Results for DOG 6

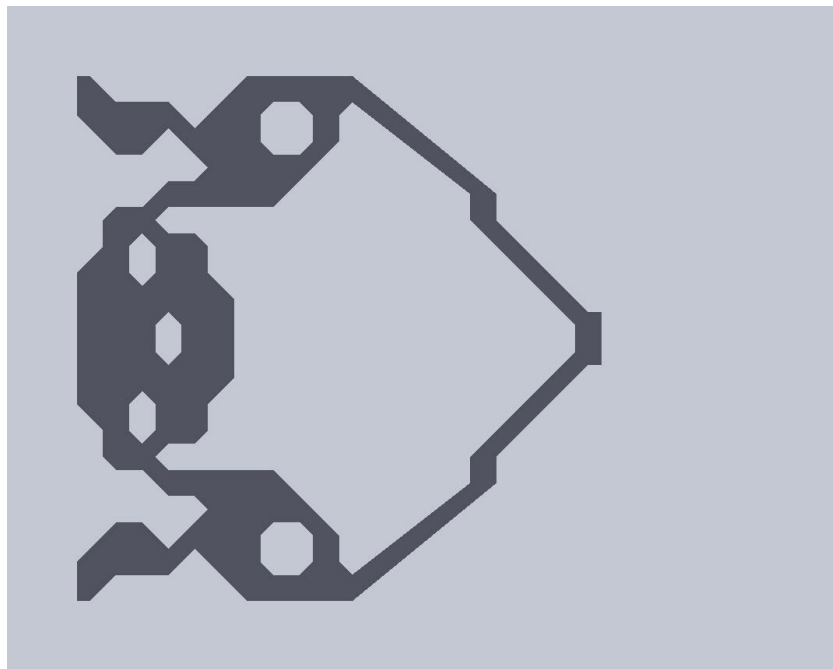


Figure 6.7 The topology with DOG 6

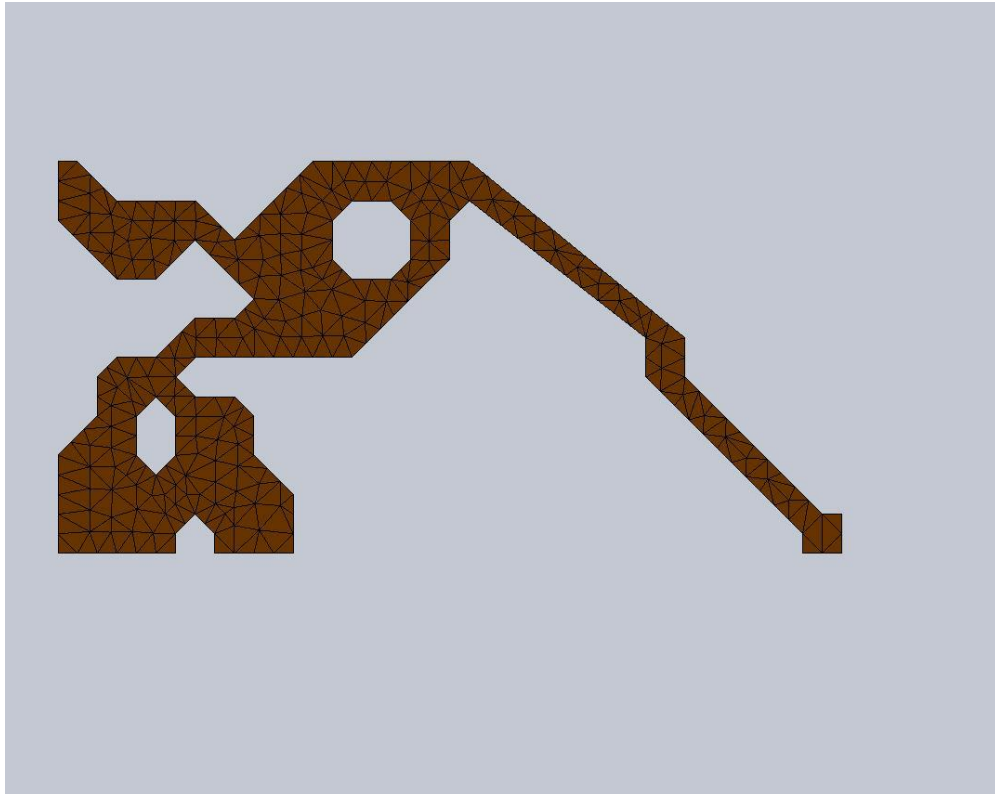


Figure 6.8 Mesh for the topology with DOG 6

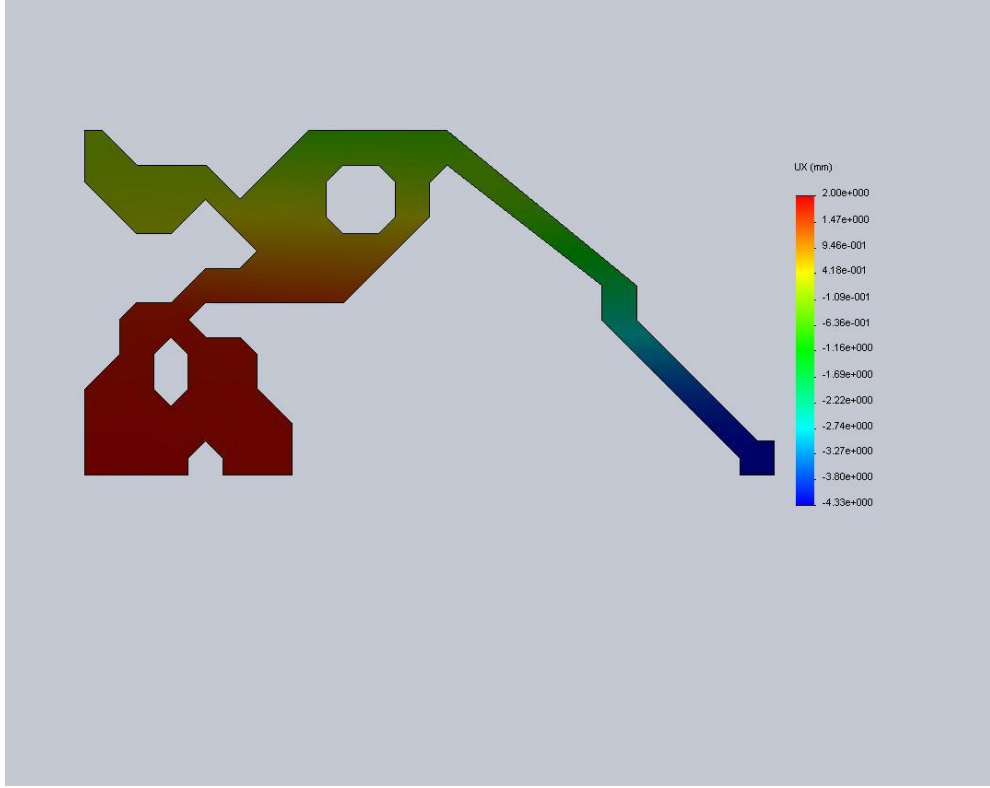


Figure 6.9 Un-deformed Displacement Distribution for topology with DOG 6

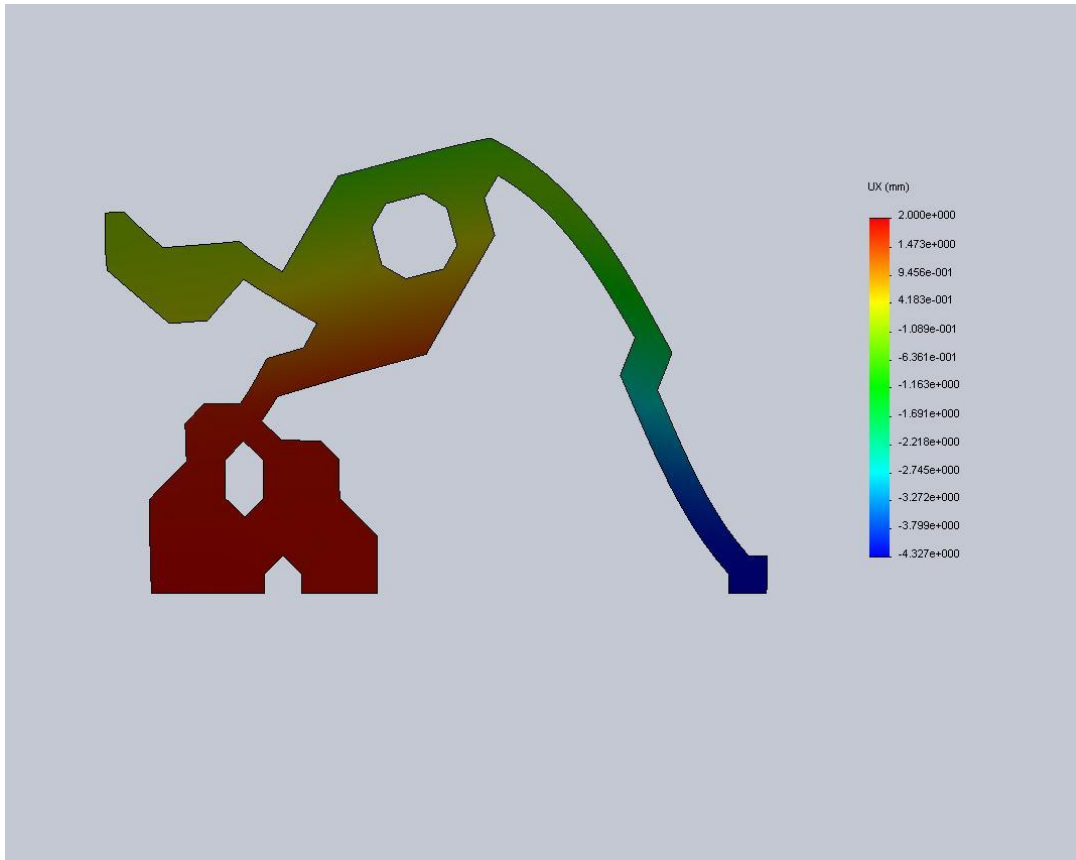


Figure 6.10 Deformed Displacement Distribution for topology with DOG 6

Table 6.3 Comparison of displacement from MATLAB and SolidWorks for DOG 6

DOG	MATLAB	SOLIDWORKS	Difference
	Displacement	Displacement	%
	(mm)	(mm)	
6	3.98	4.32	8.19

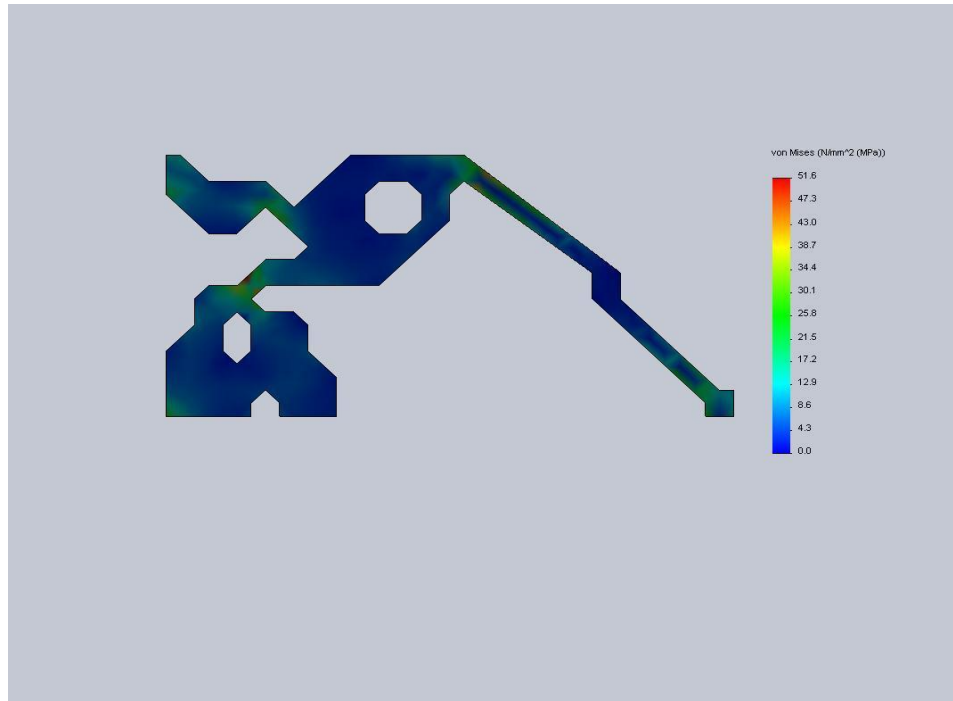


Figure 6.11 Un-deformed Stress Distribution for topology with DOG 6

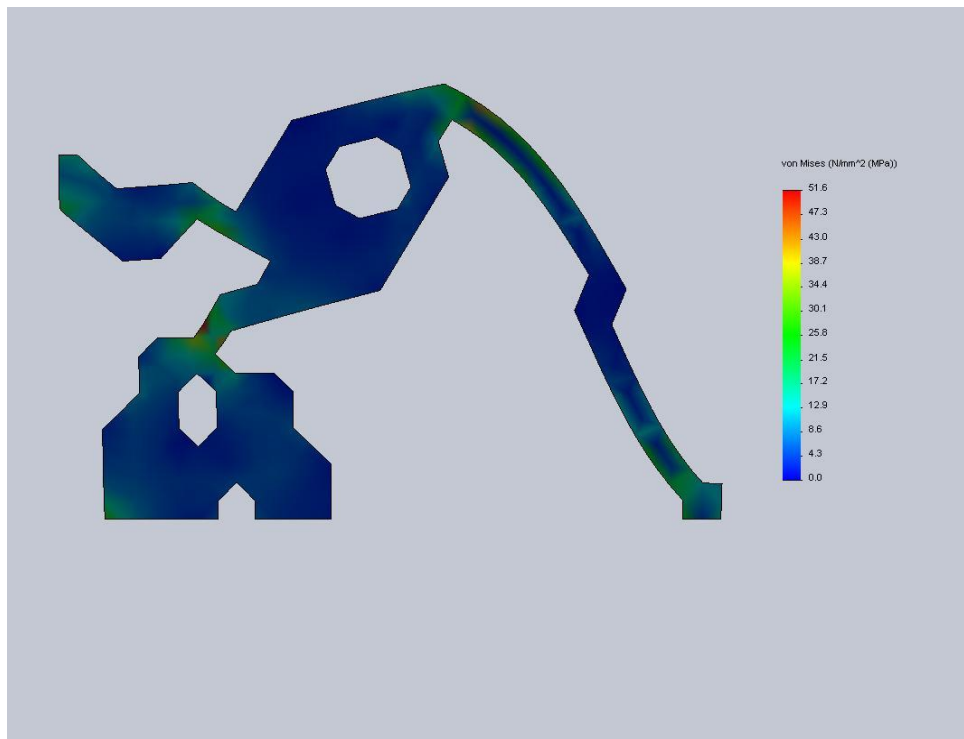


Figure 6.12 Deformed Stress Distribution for topology with DOG 6

Table 6.4 Comparison of stresses from MATLAB and SolidWorks for DOG 6

DOG	MATLAB	SOLIDWORKS	Difference %
	Stress (N/mm ²)	Stress (N/mm ²) ²	
6	53.83	51.627	-4.09

6.3 Results for DOG 7

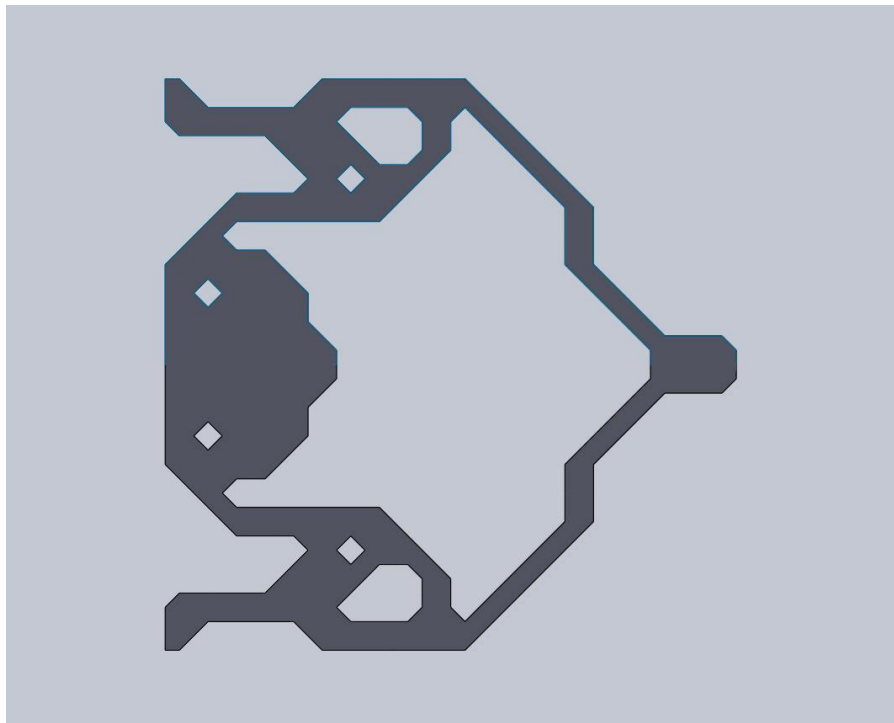


Figure 6.13 Topology with DOG 7

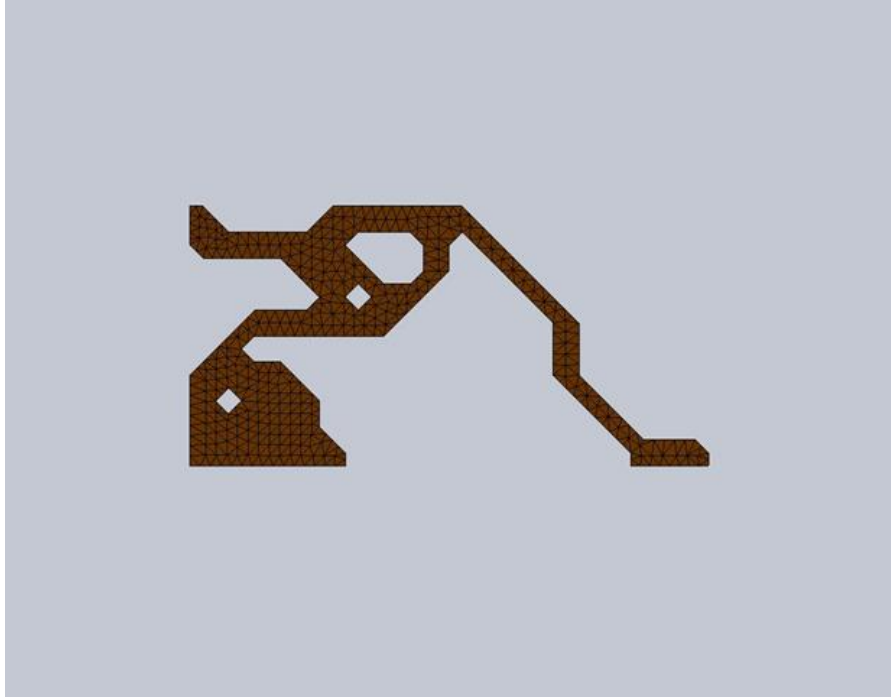


Figure 6.14 Mesh for topology with DOG 7

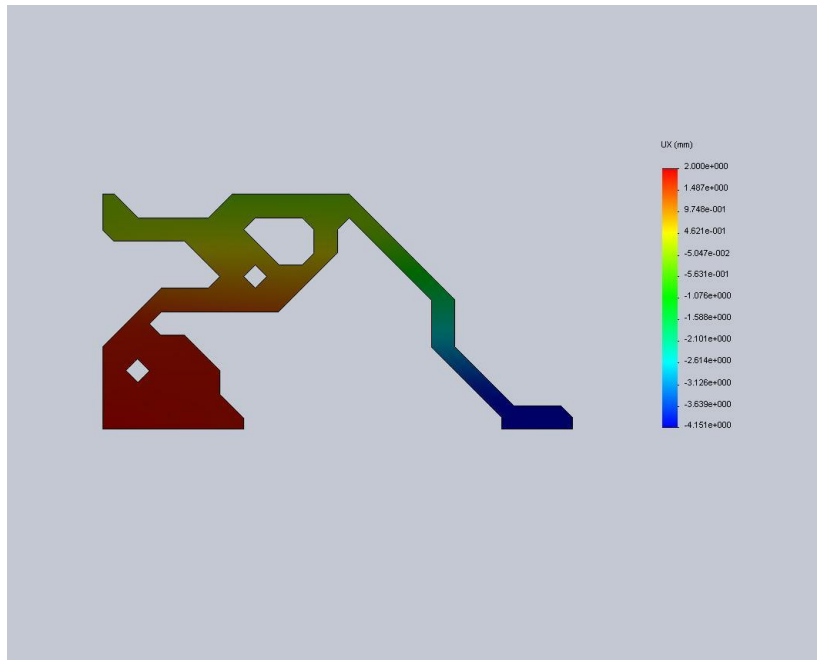


Figure 6.15 Un-deformed Displacement Distribution for topology with DOG 7

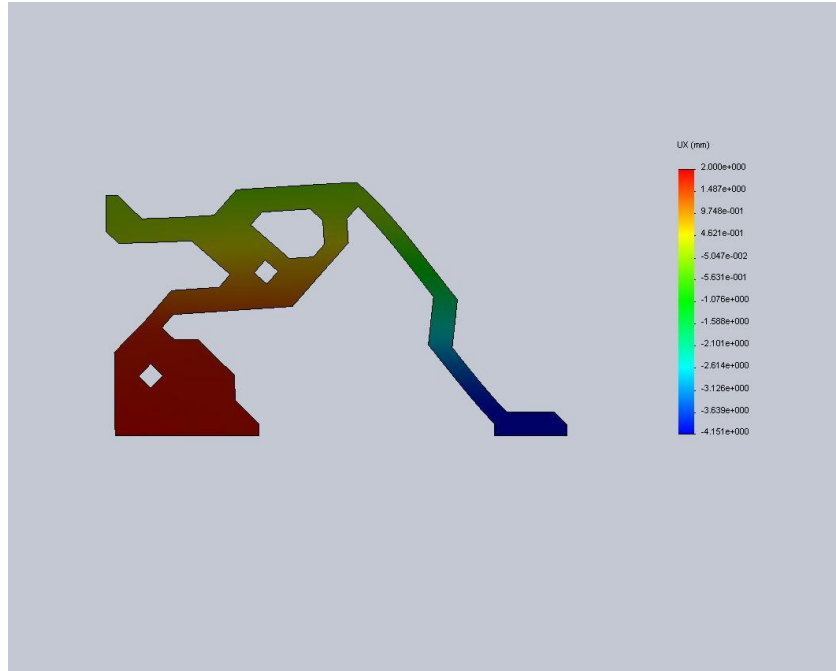


Figure 6.16 Deformed Displacement Distribution for topology with DOG 7

Table 6.5 Comparison of displacement from MATLAB and SolidWorks for DOG 7

DOG	MATLAB	SOLIDWORKS	Difference
	Displacement	Displacement	%
	(mm)	(mm)	
7	4.26	4.15	-2.28

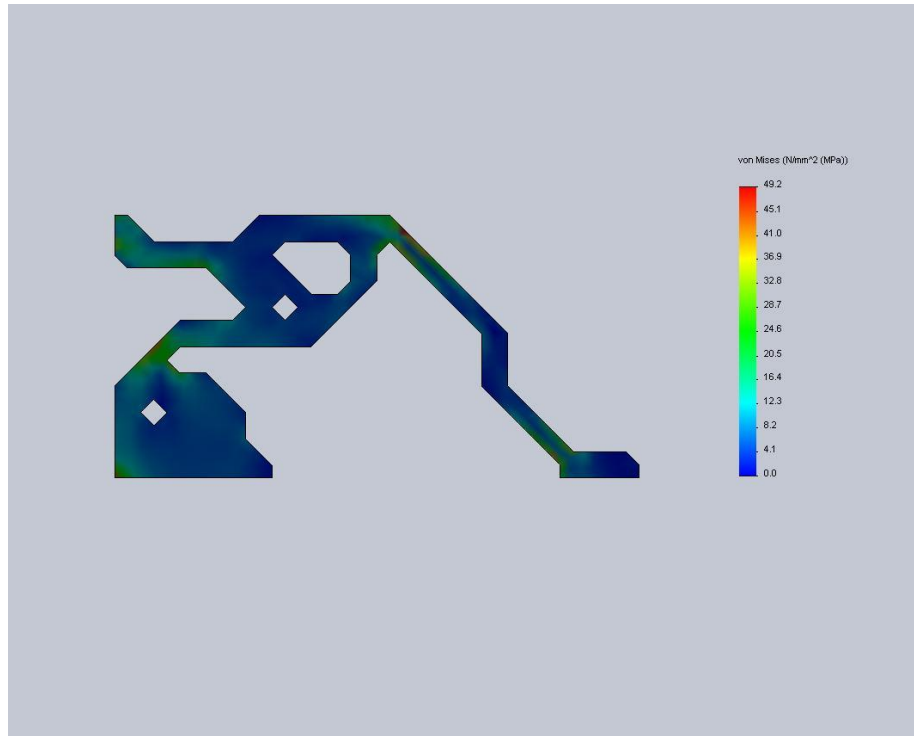


Figure 6.17 Un-deformed Stress Distribution for topology with DOG 7

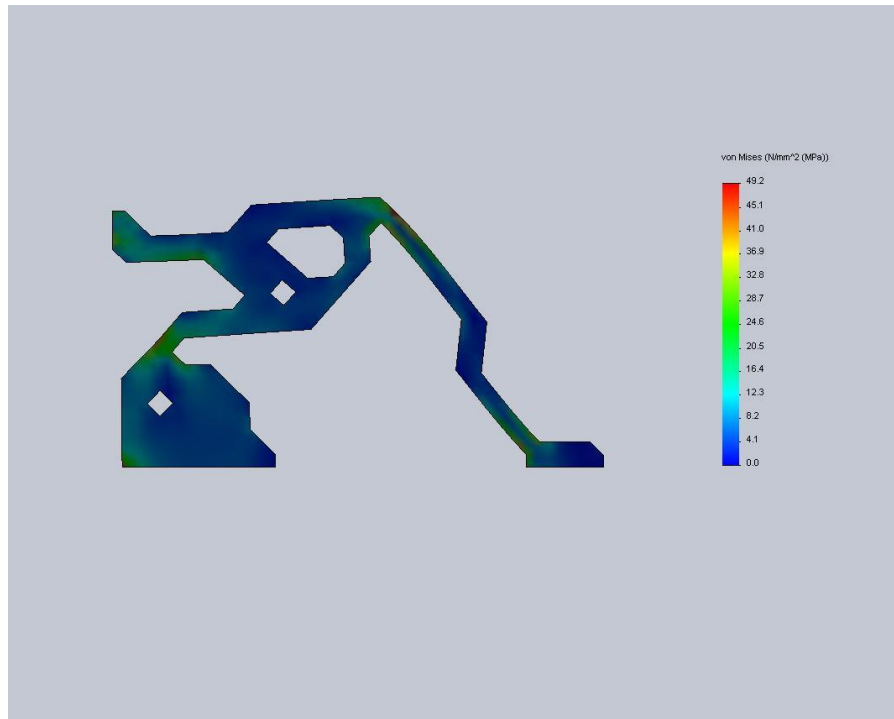


Figure 6.18 Deformed Stress Distribution for topology with DOG 7

Table 6.6 Comparison of stress from MATLAB and SolidWorks for DOG 7

DOG	MATLAB	SOLIDWORKS	Difference %
	Stress (N/mm ²)	Stress (N/mm ²) ²	
7	51.35	49.81	-2.99

6.4 Results for DOG 8

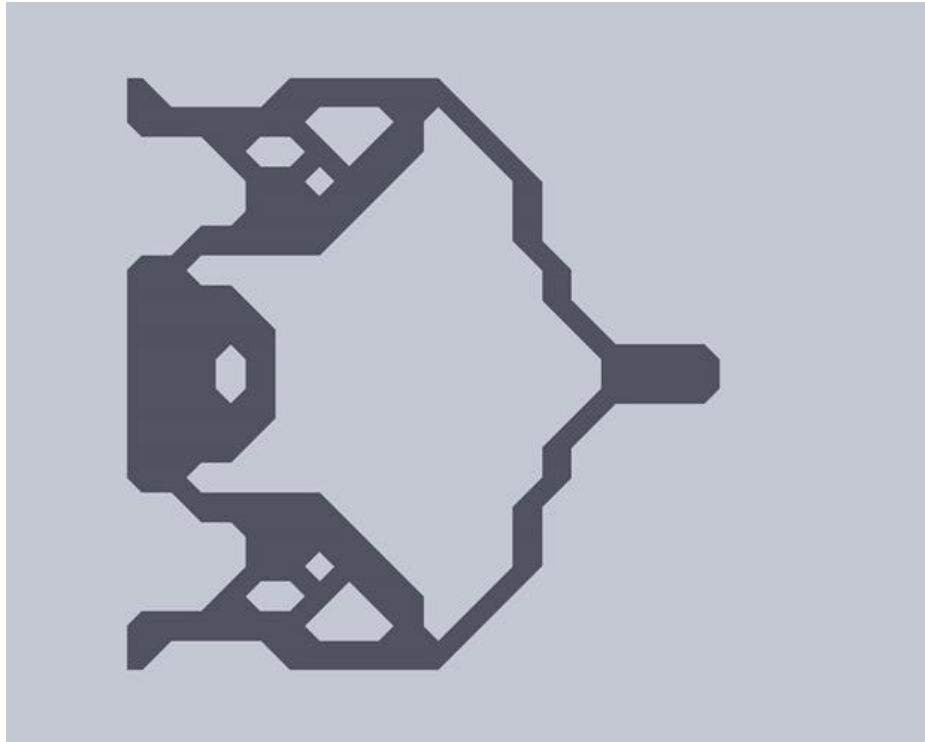


Figure 6.19 Topology with DOG 8

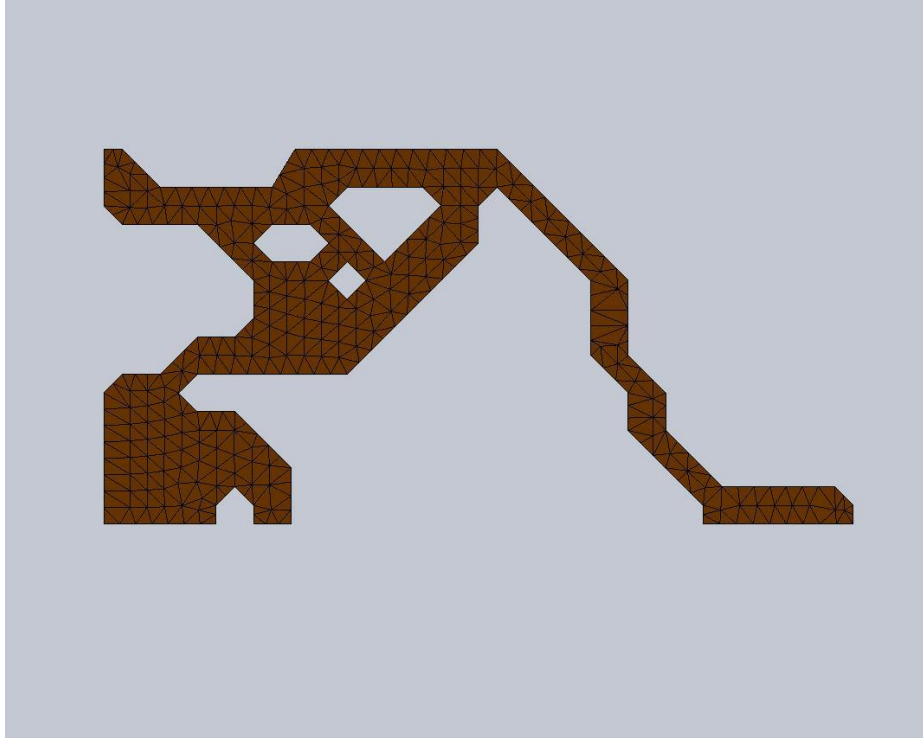


Figure 6.20 Mesh for topology with DOG 8

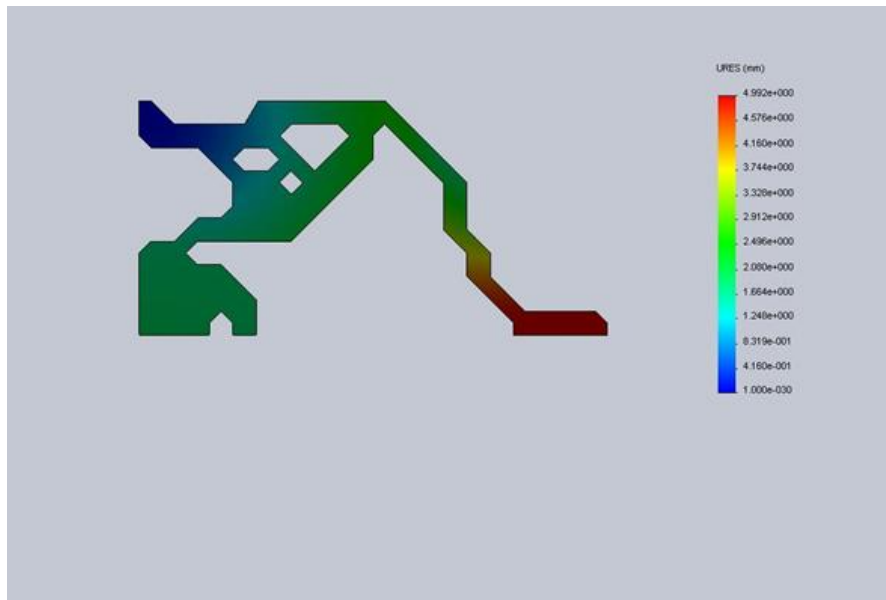


Figure 6.21 Un-deformed Displacement Distribution for topology with DOG 8

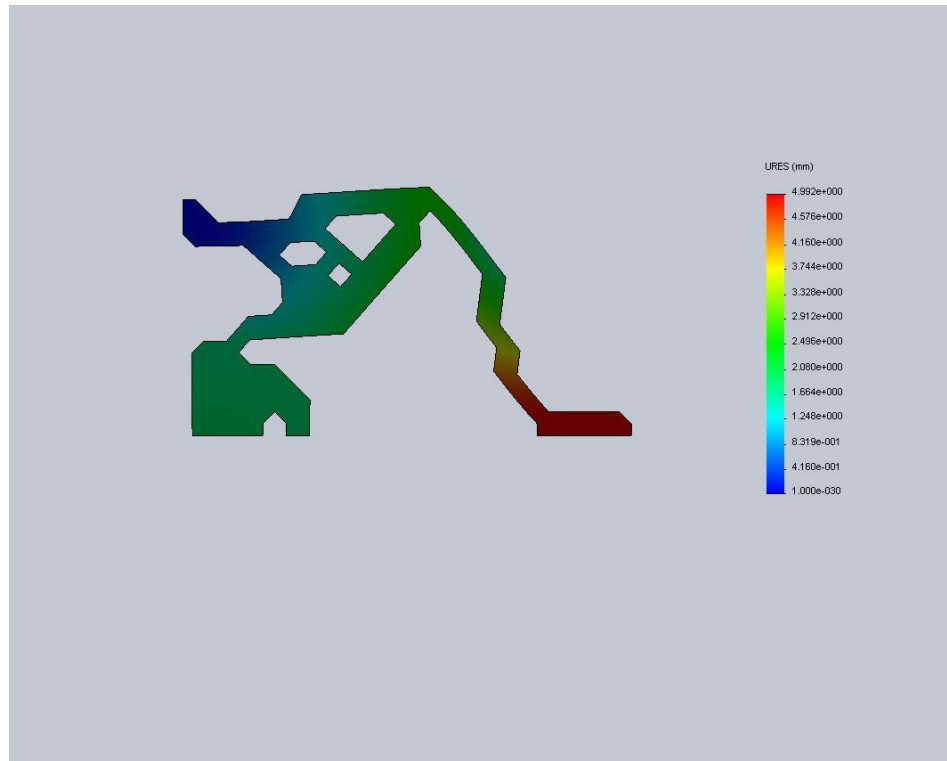


Figure 6.22 Deformed Displacement Distribution for topology with DOG 8

Table 6.7 Comparison of displacement from MATLAB and SolidWorks for DOG 8

DOG	MATLAB	SOLIDWORKS	Difference
	Displacement	Displacement	%
	(mm)	(mm)	
8	4.42	4.809	8.8

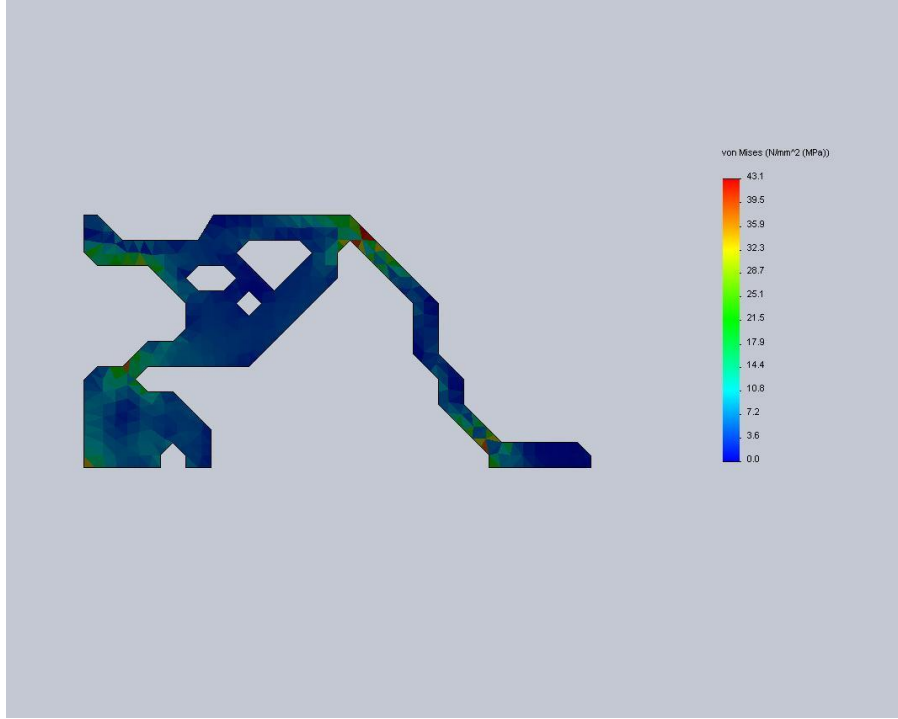


Figure 6.23 Un-deformed Stress Distribution for topology with DOG 8

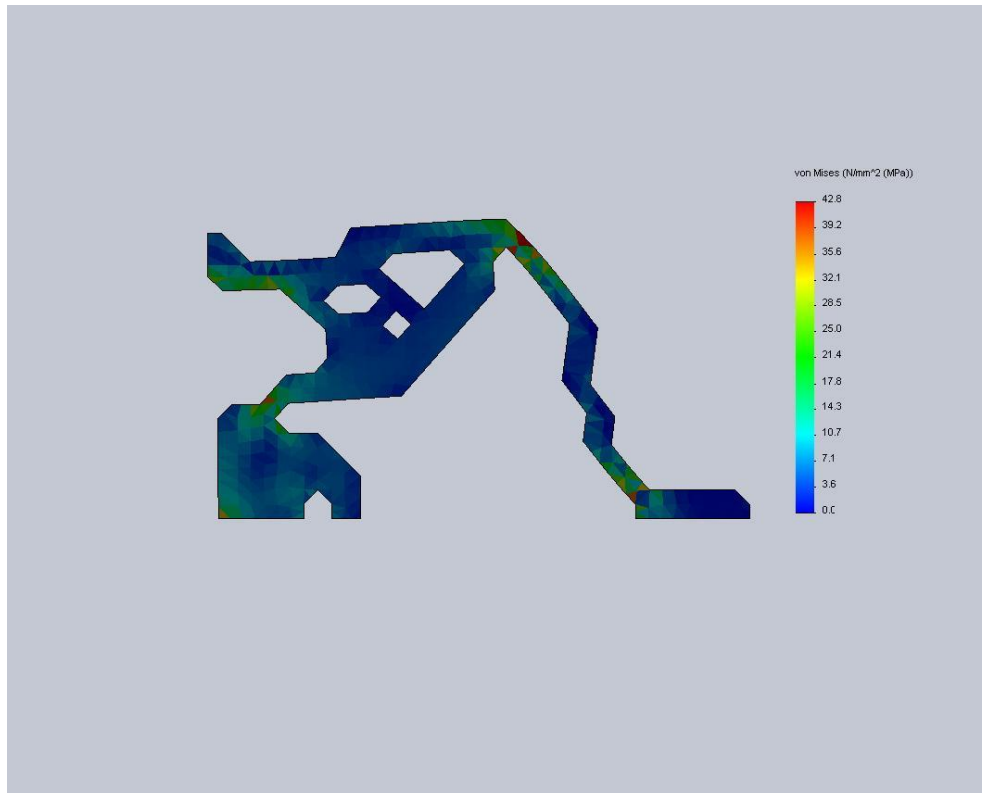


Figure 6.24 Deformed Stress Distribution for topology with DOG 8

Table 6.8 Comparison of stress from MATLAB and SolidWorks for DOG 8

DOG	MATLAB	SOLIDWORKS	Difference %
	Stress (N/mm²)	Stress (N/mm²)	
8	54.6	55.03	0.8

6.5 Results without DOG Strategy

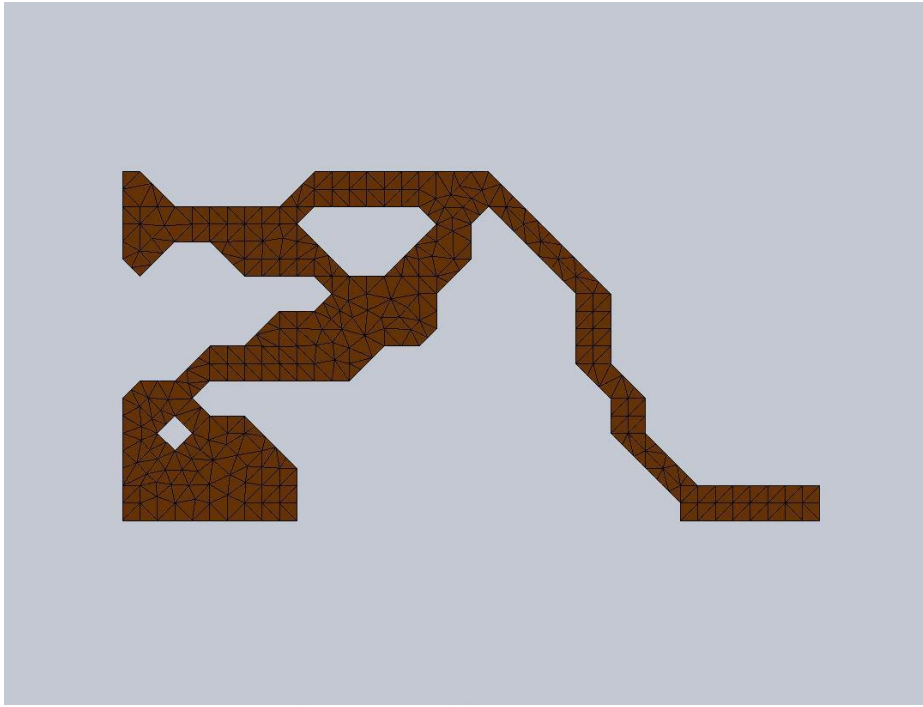


Figure 6.25 Meshing for the topology without DOG Strategy

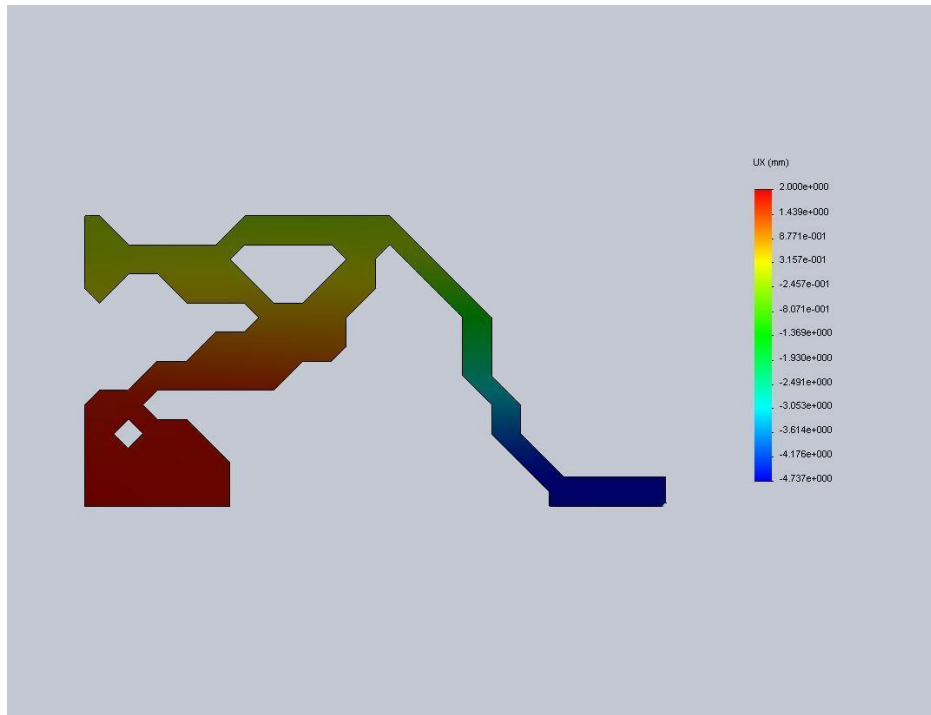


Figure 6.26 Displacement distribution for un-deformed topology without DOG strategy

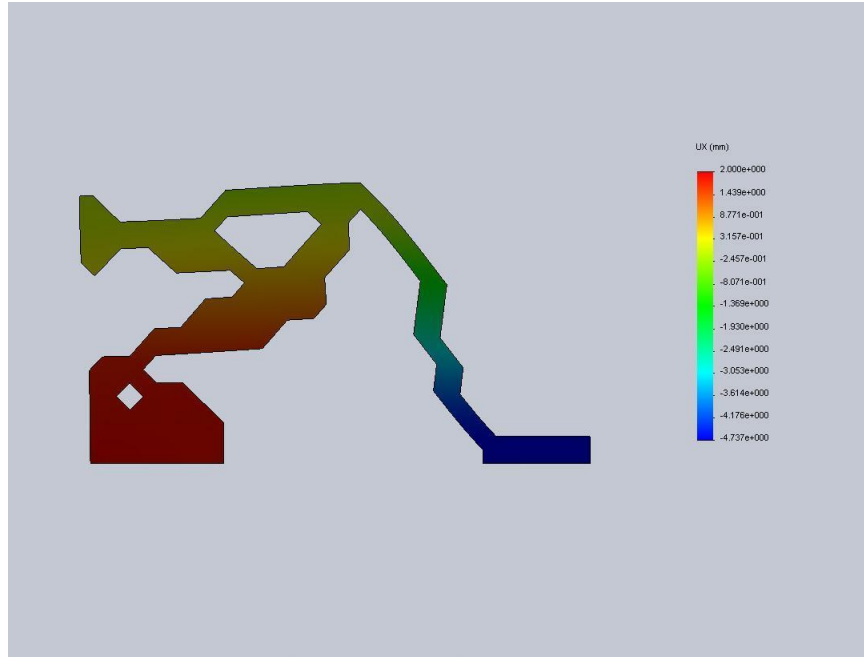


Figure 6.27 Displacement distribution for deformed topology without DOG strategy

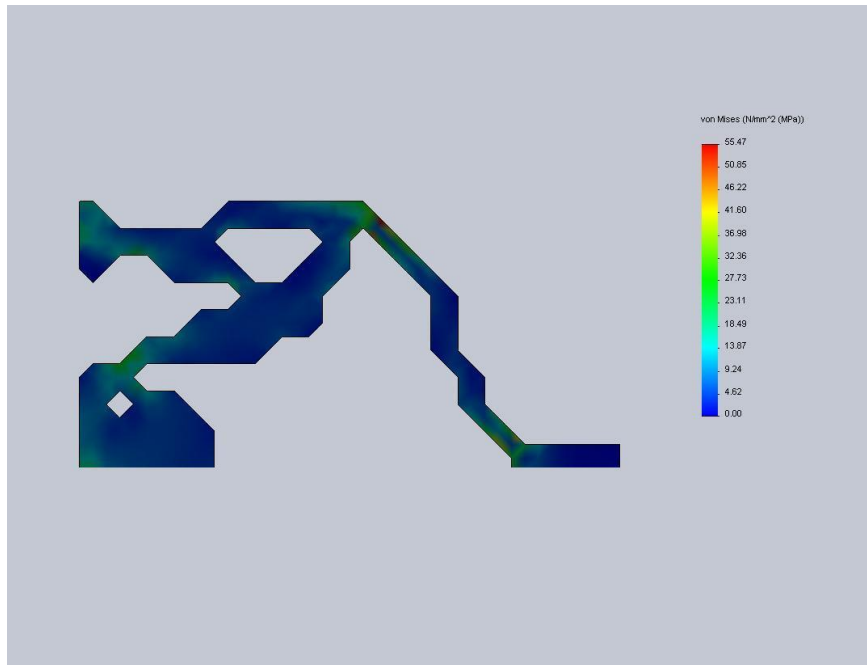


Figure 6.28 Stress distribution for un-deformed topology without DOG strategy

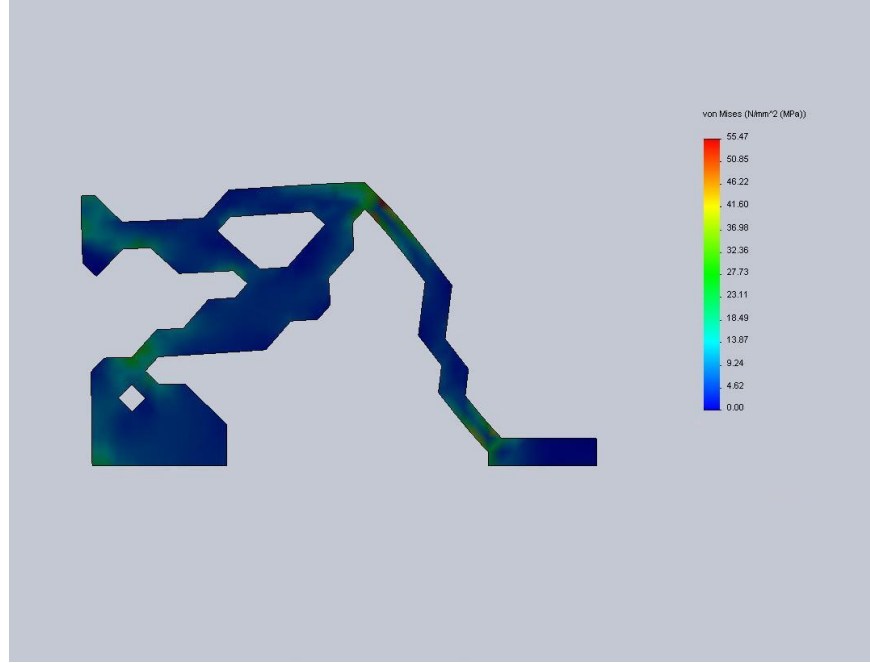


Figure 6.29 Stress distribution for deformed topology without DOG strategy

CHAPTER VII

CONCLUSIONS AND FUTURE RESEARCH

The conclusions and the future research are discussed in this chapter. The effect of the introduced strategy in eliminating the mesh dependence and the scope of future work in this area is discussed.

7.1 Conclusions

The topology solutions in this thesis are independent of the employed meshes, thus the mesh dependence problem is completely eliminated. The geometric advantage of the optimal topology of DOG 5 is 2.12 while that of the optimal topology of DOG 8 is 2.21. However the structure of the optimal topology of DOG 5 is simpler than that of the optimal topology of DOG 8. The geometric advantage of DOG 7 is 2.13, which is slightly above that of DOG 5. If DOG constraint is not considered, the optimal topology of DOG 5 has no chance to compete with that of DOG 8 or DOG 7. The choice a DOG for a mechanism is left to the designer as it can be made based on the requirements.

The chosen GA related parameters for the example like the crossover and mutation probabilities, the population size, the maximum number of generations, and the constraint violation penalty are based on the author's prior experience and there is no proof that these parameters are the best fits. To demonstrate the DOG strategy in this thesis, the population size of 150 and the maximum number of consistent 100 generations is chosen for DOGs varying from 5 through 8 and there is no guarantee that the globally optimal topology can be obtained with these choices.

7.2 Future Research

The influence on optimal topologies for different GA parameters and material volume constraints (other than 0.3) need to be further studied. Once the optimum topology is selected, it can further be optimized for its shape and stiffness using shape optimization. The DOG control strategy is introduced in this thesis to control the complexity of a synthesized distributed compliant mechanism. This strategy is also being used as the first step for circumventing the topology uncertainty caused by mesh dependence. There is much future work to improve the introduced DOG control strategy and make it more effective and efficient for topology optimization of compliant mechanisms.

REFERENCES

- [1] Zhou, H., Kandala, S.R., 2013, "The Uncertainty Elimination in Discrete Topology Optimization of Compliant Mechanisms" Proceedings of the ASME 2013 International Design Engineering Technical Conferences & Computers and Information in Engineering Conference IDETC/CIE 2013.
- [2] Saxena, A., 2008, "A Material-Mask Overlay Strategy for Continuum Topology Optimization of Compliant Mechanisms Using Honeycomb Discretization," ASME Journal of Mechanical Design, 130: (082304)1-9.
- [3] Zhou, H., 2010. "Topology Optimization of Compliant Mechanisms Using Hybrid Discretization Model," ASME Journal of Mechanical Design, 132, (111003) 1-8.
- [4] Zhou, H., Killekar, P.P., 2011, "The Modified Quadrilateral Discretization Model for the topology Optimization of Compliant Mechanisms," ASME Journal of Mechanical Design) 133, (111007) 1-9.
- [5] Norton, R. L, 2012, "Design of Machinery," McGraw-Hill, New York.
- [6] Basener, W. F., 2006, "Topology and Its Applications," Wiley, New York.
- [7] Zhou, H., Ahmed, N., Uttha, A., 2012, "The Improved Hybrid Discretization Model for the Discrete Topology Optimization of Compliant Mechanisms," Proceedings of the ASME 2012 International Mechanical Engineering Congress & Exposition, Houston, USA. IMECE2012-86181.
- [8] Deo, N., 1990, "Graph Theory with Applications to Engineering and Computer Science," Prentice Hall, Englewood Cliffs, NJ.
- [9] Block. J., 2008, "Lean Production," Industrial Press, New York.

- [10] Chapman, C. D., Saitou, K., Jakiela, M.J., 1994. "Genetic Algorithms as an Approach to Configuration and Topology Design." ASME Journal of Mechanical Design, 116: 1005-1012.
- [11] Chapman, C. D., Jakiela, M. J., 1996, "Genetic Algorithm-Based Structural Topology Design with Compliance and Topology Simplification Considerations," ASME Journal of Mechanical Design, 118: 89-98.
- [12] Kane, C., Schoenauer, M., 1996, "Topological Optimum Design Using Genetic Algorithms," Control and Cybernetics, 25: 1059-1088.
- [13] Duda, J. W., Jakiela, M. J., 1997. "Generation and Classification of Structural Topologies Genetic Algorithm Speciation," ASME Journal of Mechanical Design, 119:127-131.
- [14] Wang, S. Y., Tai, K., 2005, "Structural Topology Design Optimization Using Algorithms with a Bit-Array Representation," Computer Methods in Applied Mechanics and Engineering, 194: 3749-3770.
- [15] Tai, K., Prasad, J., 2007, "Target-Matching Test Problem for Multi objective Topology Optimization Using Genetic Algorithm for Progressive Refinement in Topology Optimization," Structural and Multidisciplinary Optimization, 34: 333- 345.
- [16] Wang, N. F., Tai, K., 2008, "Design of Grip-and-Move Manipulators Using Symmetric Path Generating Compliant Mechanisms," ASME Journal of Mechanical Design, 130: (112306) 1-9.
- [17] Wang N. F., Tai, K., 2010, "Design of 2-DOF Compliant Mechanisms to Form Grip-and-Move Manipulators for 2D Workspace," ASME Journal of Mechanical Design, 132: (031007)]-9.
- [18] Haupt, R. L. Haupt, S.E., 2004, "Practical Genetic Algorithms," 2nd ed., Wiley, New York.

VITA

Satya Raviteja Kandala received his Bachelors of Technology in Mechanical Engineering from Jawaharlal Nehru Technological University, Hyderabad, India. He is presently pursuing his Masters of Science in Mechanical engineering at Texas A&M University- Kingsville, Texas.

Permanent Address:

Dr.No : 38-30-42,

Flat 504, Sai Lakshmi Sadan,

Sai Nagar, Marripalem,

Visakhapatnam, India.